2024 2nd International Conference on Recent Trends in Microelectronics, Automation, Computing and Communications Systems (ICMACC)

2024 2nd International Conference on Recent Trends in Microelectronics, Automation, Computing and Communications Systems (ICMACC) | 979-8-3503-6657-0/24/$31.00 ©2024 IEEE | DOI: 10.1109/ICMACC62921.2024.10894457

Implementing a Deep Learning based Bridge Defect Detection System using Jetson Nano

Ranjan K. Senapati
Dept. of ECE
VNR VJIET
Hyderabad, India
ranjan_ks@vnrvjiet.in

K. Akhil Kumar
Dept. of ECE
VNR VJIET
Hyderabad, India
akhilkouda1976@gmail.com

P.M.K. Prasad
Dept. of ECE
GVPCE for Women, Madhurawada
Visakhapatnam, Andhra Pradesh, India
pmkp70@gmail.com

***Abstract*—This work describes the creation and application of an NVIDIA Jetson Nano platform-based deep learning bridge fault detection system. Bridges constitute crucial pieces of infrastructure, and maintaining safety and averting catastrophic failures depend on quick detection of flaws like corrosion, cracks, or structural damage. Conventional inspection techniques can be time-consuming, labor-intensive, and prone to mistakes. Here, we offer a computer vision-based methodology that uses deep learning techniques to automatically identify and categorize bridge structure faults from photos collected with fixed cameras or by drones. Real-time defect detection uses the NVIDIA Jetson Nano as an edge computing device because of its great computational capacity and low power consumption. The three primary phases of the suggested system include preprocessing images, employing convolutional neural networks (CNNs) for fault identification, and post-processing for analysis and visualization.**

Using the Jetson Nano's GPU acceleration for quick inference, we gathered a dataset of bridge photos with different kinds of flaws and carried out comprehensive tests to assess the system's performance. The suggested method shows efficient covering defects with an accuracy of 96%, while preserving the Jetson Nano platform's real-time processing capabilities.

***Index Terms*—Support vector machines (SVM), Convolutional neural networks (CNN), Feature engineering, Crack detection, Corrosion detection, Image segmentation**

I. Introduction

The existence of cracks is a vital safety indicator. A crack is essentially an interruption in a solid body that can occur on various surfaces, such as roads, buildings, bridges, glass, railroad tracks, pavements, cars, metals, airplanes, and tunnels. A variety of surface fractures, the crack formation can be influenced by several factors, including internal stresses inside structures, fatigue stresses, and cyclic loads. Determining the source of the crack is essential for evaluating the extent of the damage and averting prospective damage. To ensure accurate crack detection, two methods are commonly employed: A) Manual Inspection method and B) Automated Inspection method. Manual crack detection has limitations. This method is time-consuming and lacks traditionally regular manual inspection, which knowledgeable individuals conduct. The use of surveying tools and visual assessment has drawbacks. Inspectors find it difficult to access inaccessible surfaces such as tunnels, structures, and dams with this method since it is inconsistent, time-consuming, and labor-intensive. Thus, a trustworthy automated crack detection technique with excellent accuracy is required. Techniques in image processing provide a workable answer to this issue. Photographs are taken for fracture surface analysis using high-resolution cameras; greater camera resolutions improve the accuracy of the photographs. A generic architecture for an image processing technique to identify cracks consists of 1) a camera to capture the image, 2) pre-processing the image by segmenting, and scaling, which are the fundamental steps 3) different techniques to separate essential details 4) feature extraction to extract the shape of the crack. Kaan *et al.* [1], and Yun *et al.* [2] argue that using morphological and thresholding procedures with established criteria produces better results; however, fine-tuning the thresholding value is required for exact results. Acknowledging the need for a uniform thresholding technique, efforts are focused on improving it. Furthermore, edge extraction is a method that researchers favor due to its effectiveness. As a result, an algorithm for thresholding automatically is developed, which allows for smooth operation with similar sample types. Bridge photos may be used to extract important information by using image processing techniques, such as locating structural abnormalities including corrosion, cracks, and deformations. These methods could include pre-processing stages that aid in identifying and examining areas of interest within the photos, like feature extraction, segmentation, and image enhancement. There are various stages based on the input given. By identifying patterns and characteristics typical of many kinds of bridge faults, machine learning methods are essential to automate the defect identification process. Convolutional neural networks (CNNs) and support vector machines (SVMs) are two supervised learning techniques that may trained on labeled datasets that include examples of both good and bad bridge photographs. The algorithms can accurately classify and locate problems through this approach.

A. Related Work

Sergio Ruggieri *et al.* [3] presented a study about defect detection on structural elements of existing bridges through a machine learning approach. The proposed methodology aims to explore the possibility of automatically recognizing defects and damages on bridges by employing a training of existing convolutional neural networks on a set of photos.

2024 2nd International Conference on Recent Trends in Microelectronics, Automation, Computing and Communications Systems (ICMACC)

2024 2nd International Conference on Recent Trends in Microelectronics, Automation, Computing and Communications Systems (ICMACC) | 979-8-3503-6657-0/24/$31.00 ©2024 IEEE | DOI: 10.1109/ICMACC62921.2024.10893897

Real-Time Compressed Domain Face Recognition Using Deep Learning

Ranjan K Senapati
Dept of ECE
VNRVJIET, Bachupally
Nizampet,Hyderabad,India
ranjan_ks@vnrvjiet.in

Indhu Gondra
Dept of ECE
VNRVJIET, Bachupally
Nizampet,Hyderabad,India
indhugondra@gmail.com

Pragna Panyala
Dept of ECE
VNRVJIET, Bachupally
Nizampet,Hyderabad,India
pragna.panyala@gmail.com

PMK Prasad
Dept of ECE
GVPCE for Women, Madhuravada
Vishakapatnam,Andra Pradesh,India
pmkp70@gmail.com

***Abstract* — The growing demand for facial recognition systems necessitates efficient processing of images, particularly in resource-constrained environments. Compressed images offer a significant advantage in terms of storage and transmission bandwidth, but traditional face recognition algorithms struggle with the information loss inherent in compression techniques like JPEG. This paper explores the feasibility of using a VGG-16 based approach for real-time face recognition directly in the compressed domain.**

We leverage transfer learning by fine-tuning a pre-trained VGG-16 model on a dataset of compressed facial images. This approach capitalizes on the powerful feature extraction capabilities of VGG-16 while adapting it to the challenges of compressed images, such as artifacts and information loss. Our evaluation demonstrates that the trained model achieves accurate face recognition using compressed images, paving the way for real-world applications with bandwidth and storage limitations. Future work could involve exploring the impact of different compression techniques on recognition accuracy and potentially improving robustness against compression artifacts.

This work acknowledges the inherent trade-off between the compression ratio of images and the achievable recognition accuracy. In this thesis, we are investigating this relationship to identify the optimal balance between storage efficiency and recognition performance for real-world deployments.

Keywords* — *Deep learning*, *VGG-16, Compressed images, facial recognition, transfer learning

I. Introduction

The burgeoning demand for real-time face recognition systems in various domains, including security, access control, and human-computer interaction, underscores the necessity for robust and efficient solutions. However, this need is compounded when faced with the challenge of operating in environments where image data is compressed to conserve storage and bandwidth. Compression algorithms, while beneficial for reducing data size, often introduce artifacts that can compromise the fidelity of facial features crucial for accurate recognition. Traditional feature extraction methods, ill-equipped to handle these distortions, struggle to maintain recognition accuracy in such scenarios.

In response to this pressing challenge, this research embarks on an exploration of utilizing the VGG-16 deep learning model for real-time face recognition in compressed domains. VGG-16, a pre-trained convolutional neural network (CNN) renowned for its success in image classification tasks, emerges as a promising candidate for adapting to the intricacies of compressed image data. Our investigation focuses on achieving two primary objectives:

A. Superior Recognition Accuracy:

Deep learning models, exemplified by VGG-16, possess the capability to learn intricate, hierarchical feature representations from images. This innate capacity enables them to achieve markedly higher recognition accuracy compared to conventional methods, even when operating on compressed images replete with artifacts.

B. Real-Time Processing Speeds:

While deep learning offers unparalleled accuracy, ensuring real-time performance presents a formidable challenge. This research delves into techniques aimed at optimizing the VGG-16 model for expedited processing without compromising recognition accuracy. Such optimization is imperative for real-world applications necessitating swift face recognition within constrained timeframes.

By leveraging the strengths of deep learning with the VGG-16 architecture, this research aims to pioneer a solution that marries high accuracy with real-time suitability for practical face recognition scenarios involving compressed images. This research heralds a departure from traditional methods, foregrounding deep learning with VGG-16 as a paradigm shift poised to deliver superior performance in real-time settings.

II. Literature Review

Face recognition, a pivotal aspect of biometric identification, has garnered considerable attention in recent years owing to its wide-ranging applications across diverse domains. This literature review endeavors to provide a comprehensive overview of existing research endeavors, focusing on methodologies, techniques, and advancements pertinent to face recognition using compressed images.

C. Ranjeeth Kumar *et al.* [1] proposed face recognition utilizing convolutional neural networks (CNNs) and Siamese networks, showcasing notable success in face recognition tasks and laying the groundwork for further exploration into sophisticated deep learning techniques for image analysis. In a similar vein, Anwarul *et al.* [2] present a novel hybrid ensemble convolutional neural network for face recognition by optimizing hyperparameters, demonstrating advancements in model optimization techniques.

5G and IoT for Next Generation Connectivity through Enhanced Network Performance and Seamless Integration

AMIT JOSHI

Dr. PIYUSH CHARAN

Mrs. N. RAMYA

Dr. RAVI M YADAHALLI

RAD
Emics

RAD
Emics

India | Brazil | Kenya

1ST Edition – 2024

ISBN 978-81-979336-3-9

Price - INR ₹ 800 | USD $10

Head office -Saravanampatti

Coimbatore, India

Dedicated to our family members.

Contents

Chapter 10

Edge Computing in 5G and IoT Enhancing Data Processing Real-Time Analytics and Reducing Latency for Critical Applications

Dr. Raj Kumar Goswami, Professor, Department of Electronics and Communication Engineering, Gayatri Vidya Parishad College of Engineering for Women (Autonomous), Visakhapatnam Andhra Pradesh, India, rajkumargoswami@gmail.com

Dr. Ganesh Laveti, Associate Professor, Department of Electronics and Communication Engineering, Gayatri Vidya Parishad College of Engineering for Women (Autonomous), Visakhapatnam Andhra Pradesh, India, ganeshlaveti2010@gvpcew.ac.in

Abstract

The integration of 5G networks, edge computing, and Internet of Things (IoT) was transforming the landscape of modern digital systems, enabling more efficient, scalable, and responsive applications across various sectors. This chapter explores the synergies between these technologies, focusing on their role in enhancing real-time data processing, reducing latency, and optimizing bandwidth for critical applications. The convergence of 5G and edge computing plays a pivotal role in addressing the limitations of traditional cloud-based systems by enabling localized data processing, which was crucial for applications in smart cities, healthcare, precision agriculture, and autonomous systems. By enabling ultra-low latency communication and supporting massive device connectivity, these technologies ensure seamless interaction between edge devices and IoT networks, paving the way for advanced real-time analytics and decision-making. However, challenges related to infrastructure deployment, security, and scalability remain key areas of ongoing research. This chapter also outlines future directions for the continued evolution of these technologies, highlighting their potential in emerging fields such as augmented reality (AR), virtual reality (VR), and smart manufacturing. The insights provided are crucial for understanding the transformative impact of 5G and edge computing on critical applications in a data-driven world.

Keywords:

5G Networks, Edge Computing, Internet of Things (IoT), Real-Time Data Processing, Latency, Real-Time Analytics

Introduction

The convergence of 5G networks, edge computing, and the IoT represents a significant leap forward in the capabilities of modern digital ecosystems [1,2]. As industries strive for greater connectivity and intelligence, the demand for faster, more scalable, and responsive systems has become paramount [3]. The combination of 5G's high-speed connectivity, edge computing's localized processing, and IoT's ability to interconnect devices creates a powerful infrastructure that can support the next generation of critical applications across various sectors [4]. This chapter examines the intersection of these

THE ART OF DESIGN THINKING

(PROBLEM TO PROTOTYPE)

Dr. Raj Kumar Goswami

IDEA

SAN INTERNATIONAL
SCIENTIFIC PUBLICATIONS

THE ART OF DESIGN THINKING
(Problem to Prototype)

Author

Dr. Raj Kumar Goswami
Professor and Principal
Gayatri Vidya Parishad College of Engineering for Women
Visakhapatnam, India.

SAN INTERNATIONAL
SCIENTIFIC PUBLICATIONS

THE ART OF DESIGN THINKING
(Problem to Prototype)

(**Author**: Dr. Raj Kumar Goswami)

ISBN: 978-81-972500-9-5
DOI: https://doi.org/10.59646/adt/181

Edition 1: April 2024

Published by

San International Scientific Publications
Email: editor@nobelonline.in
Website: sanpublications.nobelonline.in

DATA & INFORMATION SECURITY

Dr. RAJ KUMAR GOSWAMI
Mrs. S. NANDHINI DEVI
Dr. SHWETA A. BANSAL
Mrs. PUSHPA PRASANNA

SAN INTERNATIONAL
SCIENTIFIC PUBLICATIONS

DATA & INFORMATION SECURITY

Authors

Dr. Raj Kumar Goswami
Professor and Principal
Gayatri Vidya Parishad College of Engineering for Women, Visakhapatnam, India.

Mrs. S. Nandhini Devi
Assistant Professor, Department of MTECH- CSE,
Sri Sairam Engineering college, West Tambaram,
Chennai, Tamil Nadu, India.

Dr. Shweta A. Bansal
HOD and Associate Professor,
Department of CSE, K R Mangalam University,
India

Mrs. Pushpa Prasanna
Assistant Professor, Department of CSE,
RP Sarathy Institute of Technology, Salem,
Tamilnadu, India

SAN INTERNATIONAL
SCIENTIFIC PUBLICATIONS

DATA & INFORMATION SECURITY

(Authors: Dr. Raj Kumar Goswami, Mrs. S. Nandhini Devi, Dr. Shweta A. Bansal and Mrs. Pushpa Prasanna)

ISBN: 978-81-964397-4-3

Published by

San International Scientific Publications
Email: editor@nobelonline.in
Website: sanpublications.nobelonline.in

Publisher's Disclaimer

The Publisher of this book states that the Authors of this book has taken the full responsibility for the content of this book, any dispute and copyright violation arising based on the content of this book will be addressed by the editor(s), furthermore, the authors indemnify the publisher from damages arising from such disputes and copyright violation as stated above.

MOBILE AND CELLULAR COMMUNICATION

(Including 5G & Beyond and Microstrip Antennas)

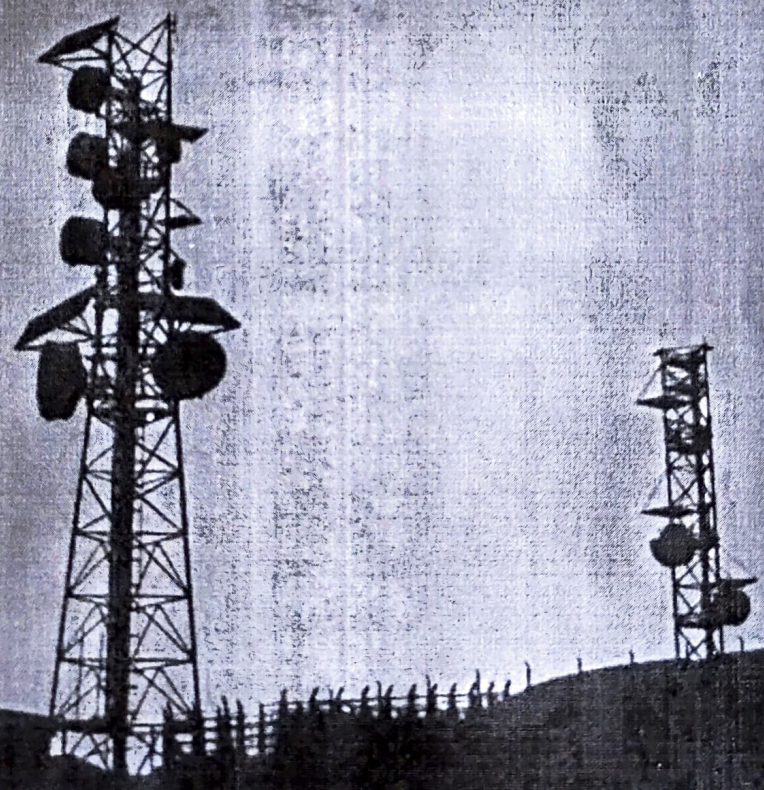

Prof. Gottapu Sasibhushana Rao
Prof. Raj Kumar Goswami
Prof. M.N.V.S.S Kumar

MOBILE AND CELLULAR COMMUNICATION

(Including 5G & Beyond and Microstrip Antennas)

Prof. Gottapu Sasibhushana Rao
Prof. Raj Kumar Goswami
Prof. M.N.V.S.S Kumar

PARAMOUND BOOK DISTRIBUTORS
Delhi • Visakhapatnam

PARAMOUND BOOK DISTRIBUTORS
B-61/E-1, Gali No. 14, Jagatpuri Ext.
Shahdara, Delhi-110093
Mobile: 9868320502, 8247897557, 9030046333
E-mail: pbookdistributors@gmail.com

Branch Office:
Office #28-8-3, 1st Floor
Opp Sri Venkateswara Theatre Out Gate
Sryabagh, Visakhapatnam
Ph.: 0891-6639247, 6654633

MOBILE AND CELLULAR COMMUNICATION
(Including 5G & Beyond and Microstrip Antennas)

First Edition 2024

ISBN 978-81-967696-8-0

PRINTED IN INDIA

Published by Paramound Book Distributors and Printed at Global Printers, Delhi.

Tamper Localization through Fragile Watermarking with Vigenère Cipher Encryption

1st Ranjan K Senapati
Dept of ECE
VNRVJIET, Bachupally
Nizampet, Hyderabad, India
ranjan_ks@vnrvjiet.in

2nd Indhu Gondra
Dept of ECE
VNRVJIET, Bachupally
Nizampet, Hyderabad, India
indhugondra@gmail.com

3rd Pragna Panyala
Dept of ECE
VNRVJIET, Bachupally
Nizampet, Hyderabad, India
pragna.panyala@gmail.com

4th Pranav J
Dept of ECE
VNRVJIET, Bachupally
Nizampet, Hyderabad, India
20071A0445@vnrvjiet.in

5th V. Sagar Reddy
Dept of ECE
VNRVJIET, Bachupally
Nizampet, Hyderabad, India
sagarreddy_v@vnrvjiet.in

6th P. M. K. Prasad
Dept of ECE
GVPCE for Women, Madhurawada
Visakhapatnam, Andhra Pradesh, India
pmkp70@gmail.com

2024 International Conference on Distributed Computing and Optimization Techniques (ICDCOT) | 979-8-3503-8295-2/24/$31.00 ©2024 IEEE | DOI: 10.1109/ICDCOT61034.2024.10515742

***Abstract*—The primary objective of this paper is to detect and locate alterations in digital images to ensure their tamper-proofing. To achieve this, a fragile watermarking technique has been employed and the obtained watermark has been encrypted using the Vigenère Cipher/Playfair. This versatile technique can be applied to both grayscale and colour images, focusing on spatial domain watermarking. In the proposed approach, replace the Least Significant Bits (LSBs) of the host image's pixels have been replaced with the encrypted watermark data. Authentication involves extracting the watermark from the watermarked image and comparing it with the original watermark. This Python-based implementation of Fragile Watermarking is subjected to various typical attacks on watermarked images to assess its performance. Experimental results demonstrate that the watermarked images show PSNR over 55 dB, and SSIM over 0.99 for a standard set of images, indicating the method's effectiveness in detecting image integrity in the presence of these attacks.**

Keywords—Spatial domain watermarking, Tamper detection, localization, Vigenère cipher, Fragile watermarking

I. Introduction

It's crucial to ensure that digital images remain unaltered and tamper-proof, especially in fields like journalism, law enforcement, and evidence authentication. Detecting and pinpointing unauthorized modifications within images is essential for maintaining trust and credibility in the digital world.

This paper focuses on tamper detection and localization in digital images by using an innovative approach known as Fragile Watermarking. Fragile Watermarking is a specialized form of digital watermarking that is highly sensitive to even the smallest changes made to the host image. This heightened sensitivity is achieved by encrypting a watermark using methods like the Vigenère Cipher/Playfair cipher and with the dimensions of the host image. Importantly aligning it precisely, this technique is versatile and can be applied to both grayscale and colour images, making it adaptable to a wide range of applications.

The core methodology involves replacing the Least Significant Bits (LSBs) of the host image's pixels with the encrypted watermark data. By subsequently extracting and comparing this watermark with the original, tampered regions within the image can be reliably detected and located.

Through Python-based implementation, the performance of this Fragile Watermarking technique has been assessed under various typical attacks on watermarked images. The outcomes of this paper not only contribute to the field of image integrity and security but also provide a practical tool for safeguarding digital images against unauthorized alterations.

II. Literature Review

In the realm of digital image forensics, various watermarking techniques have been developed to address the challenge of detecting and localizing tampered regions. These techniques aim to ensure the integrity and authenticity of visual content, especially in the face of evolving tampering methods and emerging threats.

Neena Raj and Shreelekshmi [1] proposed a fragile watermarking scheme utilizing Singular Value Decomposition (SVD) and logistic map for tamper localization. Their scheme achieves precise tamper localization under various attacks such as copy-paste and content removal, showcasing competitiveness against state-of-the-art algorithms. Despite its effectiveness, concerns arise regarding its vulnerability to cryptographic attacks. Ahmad and Khursheed [2] presented a tamper detection and localization model utilizing various features and optimized CNN. While achieving enhanced tamper detection accuracy, its computational complexity remains a concern. Zhang et al. introduced EditGuard [3], a proactive framework integrating copyright protection with tamper-agnostic localization. EditGuard balances tamper localization accuracy, copyright recovery precision, and generalizability to AIGC-based tampering methods. However, its scalability and performance under evolving threats warrant further exploration.

Lin et al. proposed a fragile watermarking scheme [4] utilizing AMBTC and VQ for tamper localization and self-recovery. Their approach demonstrates robustness against cutting and copy-paste attacks while maintaining high tamper localization accuracy. However, the reliance on compression methods may introduce artifacts affecting watermark robustness. Bhalerao et al. [5] presented a secure and efficient fragile image watermarking technique based on spatial domain, block-based embedding using the Secure Hashing Algorithm (SHA-1). Their approach aims to detect image tampering and localize tampered regions with high accuracy, albeit with concerns regarding SHA-1 hashing vulnerability. Ahmadi et al. [6] presented a blind dual watermarking scheme for color images, achieving high robustness and tamper localization accuracy. However, its computational complexity and potential impact on image quality require further investigation. Other novel approaches to fragile watermarking

CHAPTER 16

Navigation Autonomy: Challenges and opportunities in autonomous vehicle communication

Dr. Raj Kumar Goswami[1] and Kinjal Goswami[2]

[1]Professor, Department of Electronics and Communication Engineering, Gayatri Vidya Parishad College of Engineering for Women, Madhurwada, Visakhapatnam, Andhra Pradesh, India.
[2]Assistant Professor, Department of Computer Science and Engineering, Gayatri Vidya Parishad College of Engineering for Women, Madhurwada, Visakhapatnam, Andhra Pradesh, India.

***DOI**: https://doi.org/10.59646/CompComTechC16/119*

***Accepted:** January 25, 2024, **Available online:** February 01, 2024*

***Published by:** San International Scientific Publications*

Abstract

This exploration into "Navigation Autonomy" begins with a comprehensive overview of the evolutionary trajectory of autonomous vehicles, emphasizing the pivotal role of communication in enabling navigation autonomy. This chapter addresses challenges and security considerations within communication networks, providing a foundation for understanding the technological infrastructure supporting navigation autonomy. Moving forward, the exploration continues with a focus on the integration of lidar, radar, and camera-based sensor systems, accompanied by discussions on sensor fusion algorithms and the role of edge computing in decentralized processing for navigation autonomy. The final stretch of the exploration shifts attention to "Cybersecurity and Future Trends," addressing threats and vulnerabilities within autonomous vehicle communication systems. It details security measures and encryption protocols, concluding with anticipation of advances in autonomous vehicle communication technology and insights into future trends that will shape the landscape of navigation autonomy.

NANOTECHNOLOGY APPLICATIONS IN VARIOUS FIELDS

Abstract

There is an enormous growth in the way we have lived over the past 75 years. Furthermore, work was transformed by two miniature discoveries. One is that using semiconductor transistor and the other one miniaturisation of VLSI microchip have revolutionized modern inventions extremely since their development. In the 1939s, they have been getting smaller and smaller. In this paper introduces contemporary trends in nanotechnology then its applications besides future scope as well as addresses the progress of our country in this emerging field.

Keywords: Nano technology,biomedical, Nano technogy application

Authors

Dr. V. Radhika
ECE Department,
Pragati Engineering College(A),
Surampalem, Affiliated to JNTUK,
Kakinada. Andhra Pradesh.
radhika.v@pagati.ac.in

Dr. B.Vijayalakshmi
ECE Department,
GVP College of Engineering for Women
AU Visakhapatnam, Andhra Pradesh
bvl@gvpcew.ac

Advancements in Multiple Input Multiple Output DC-DC Converters for Efficient DC Microgrid Integration: A Scientometric Analysis

Saikumar Puppala*
Research Scholler, Dept. of EE
National Institute of Technology,
Meghalaya, India.
pkumar@nitm.ac.in*

Piyush Pratap Singh
Assistant Professor, Dept. of EE
National Institute of Technology
Meghalaya, India.
piyushpratap.singh@nitm.ac.in.

Devendra Potnuru
Associate Professor, Dept. of EEE
GVP of Engineering for Women,
Visakhapatnam, India.
devendra.p.07@gmail.com

2024 International Conference on Smart Systems for applications in Electrical Sciences (ICSSES) | 979-8-3503-6404-0/24/$31.00 ©2024 IEEE | DOI: 10.1109/ICSSES62373.2024.10561353

***Abstract*—Integrating renewable energy sources and the demand for environmentally friendly energy solutions has led to the development of DC microgrids. These microgrids offer improved efficiency, reduced transmission losses, and increased reliability. However, the intermittent nature of renewable energy generation and unpredictable demands require power electronic converters like DC-DC converters in DC microgrids. Multiple-input multiple-output (MIMO) DC-DC converters are a potential solution to address these challenges. This paper provides the study of MIMO DC-DC Converters; the study utilized the Scopus database for bibliometric analysis and retrieval of publication documents related to the selected MIMO keyword. The Scientometric analysis was conducted using the VOSviewer software. Also, this paper provides a comprehensive overview of the latest advancements in MIMO DC-DC converters for DC microgrid applications, covering various converter topologies and performance evaluation methods.**

Keywords—MIMO DC-DC Converters, DC Microgrids, Renewable Energy Integration.

I. INTRODUCTION

In the past few years, the development of microgrids has attracted much attention and momentum due to numerous key components and reasons that have contributed to this trend. A microgrid provides electricity to a specific geographical region or community by operating independently or coordinating with the main grid. Using renewable energy sources like solar, wind, biomass and battery storage, microgrids create a reliable and sustainable energy supply[1]. Reduce emissions and promote energy security and resilience by using microgrids. In generally DC microgrids are more efficient than AC microgrids and also it offers increased reliability and resiliency, operating independently from the main power grid. They provide uninterrupted power supply even during grid failures or blackouts. DC microgrids are highly efficient, eliminating the need for energy conversion from DC to AC, resulting in reduced energy losses[2]. These benefits make DC microgrids suitable for isolated or off-grid areas, additionally, essential infrastructure needs reliable and uninterrupted power.

The main challenge of a DC Microgrid is to balance the supply and demand of electricity in a localized area. It operates on a smaller scale and uses renewable energy sources, unlike traditional power grids [3] The challenges of managing fluctuations in energy production from renewable sources like solar panels and wind turbines while meeting electricity demand without overloading the system are discussed. Integrating energy storage systems is essential for maintaining a stable and reliable power supply while storing excess energy for use during periods of low production. Implementing MIMO DC-DC converters is one approach that can be used to address and overcome these issues. Fig.1 shows the basic block diagram for MIMO DC-DC Converter. MIMO converters help manage fluctuations in energy production by dynamically allocating power from different sources based on demand. This improves the stability and reliability of the power supply by efficiently storing and using excess energy during times of low production [4].

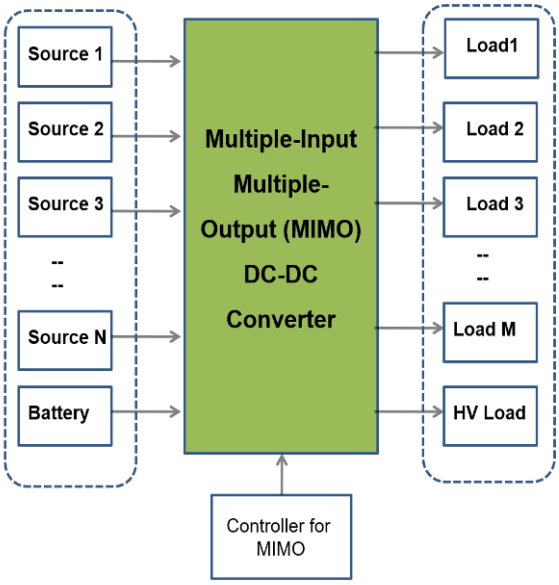

Fig. 1. Basic Block Diagram for MIMO DC-DC Converter source [5]

II. BIBLIOMETRIC ANALYSIS

Bibliometric analysis is a key part of literature review, which is a quantitative look at academic works like journals, articles, conference papers, books, and other research outputs. Bibliometric analysis illuminates the intellectual landscape, research impact, and study relationships by analysing publishing trends and citation data. The study utilized the Scopus database for bibliometric analysis and retrieval of publication documents related to the selected MIMO keyword, the Scientometric analysis was conducted using the VOSviewer software[6].

The top 118 articles have been listed from the last three years and split into this keyword from the top 10 journals with relevant MIMO keywords. Articles by the country results are shown in Fig.2. It is observed that India has published the most research articles from the last year, approximately 33 out of 118 articles, and the Documents by subject area are in the journals in Fig. 3.

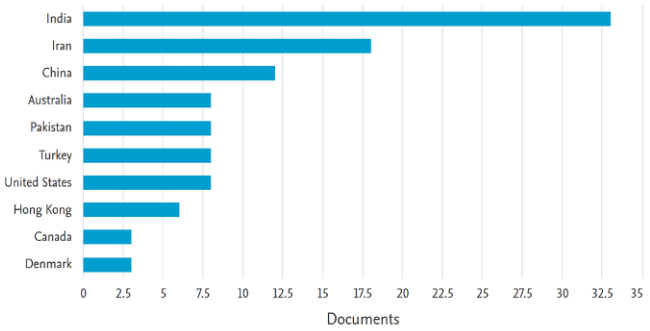

Fig. 2. Articles by the country results or territory 118 Article results

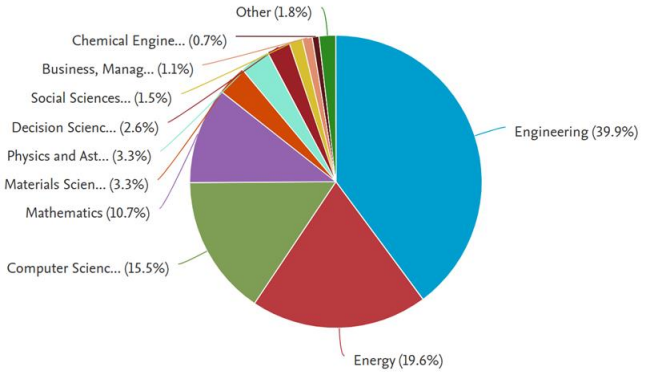

Fig.3. Documents by subject area

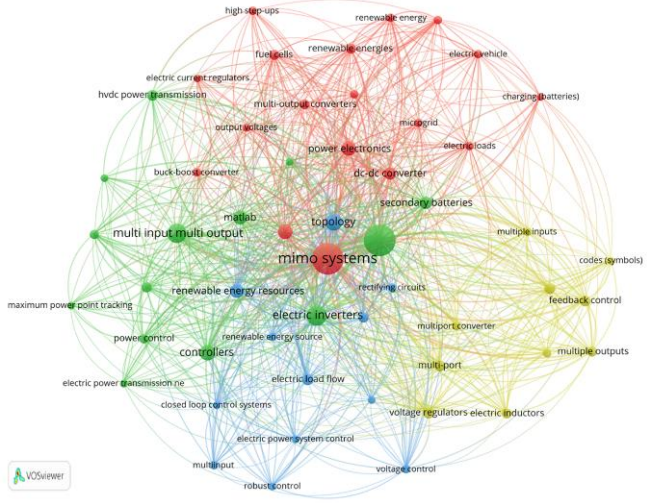

Fig.4 Network Visualization in MIMO systems key word

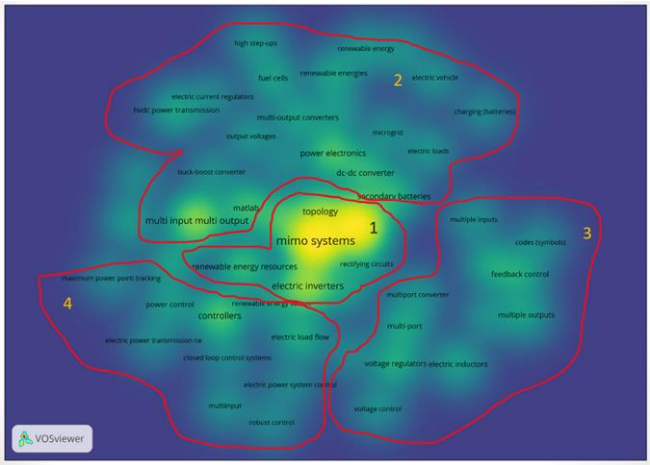

Fig. 5 Cluster Visualization in MIMO systems key word

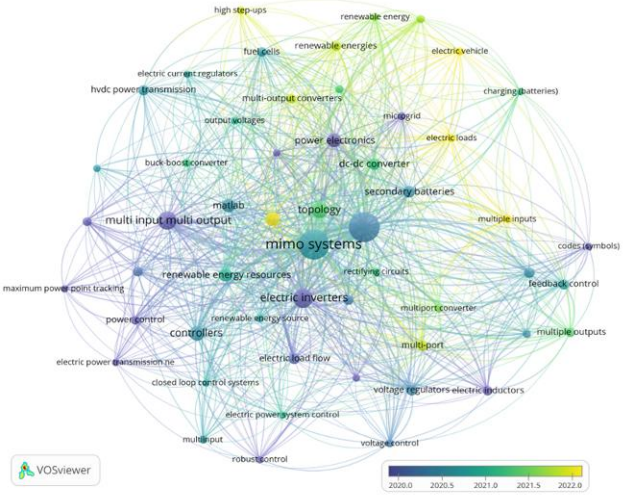

Fig. 6. Overly Visualization in MIMO systems key word

The network mapping visualization in Fig. 4 shows the occurrence weight of keywords, with MIMO being the most powerful keyword. It has 312 links and 15714 total link strength. Research studies have shown that cluster visualization effectively represents keywords, with the number of links and total link strength representing the link between keywords. The MIMO System's cluster visualization in Fig. 5 shows a total keyword divided into 4 clusters. MIMO system visualization, highlighting its potential for various applications. The lightest colour and long link distances indicate recent research and development opportunities shown in Fig. 6.

Scientometric analysis helps identify recent and future trends in MIMO System converter development, providing clear direction for related research. Overlay visualization helps bridge research gaps between keywords, while link distance and circle colour analysis helps determine future trends in related topics.

III. MIMO DC-DC CONVERTERS

Multiple-Input and Multiple-Output (MIMO) DC-DC converters, are a class of power electronic devices used to efficiently regulate and convert electrical energy between multiple input and output sources. This converter's capacity to handle power from numerous sources and distribute it to multiple loads while maximizing efficiency and performance has made it popular in many applications.

A. Classifications of MIMO MIMO DC-DC converters

MIMO DC-DC Converters can be based on various factors shown in Fig.7.

a) Converter Topology: MIMO DC-DC converters are classified based on their component arrangement, including forward, flyback, half-bridge, full-bridge, and cascaded converters. Each topology has advantages and disadvantages, making it suitable for applications and power conversion requirements. The choice depends on voltage levels, power ratings, efficiency, and cost.

b) Control Strategy: Control strategy-based classification of MIMO DC-DC Converters involves using control strategies like pulse-width modulation and phase-shift modulation to regulate the output voltage and current. These converters can achieve high efficiency and accurate

regulation by adjusting the switching frequency and duty cycle.

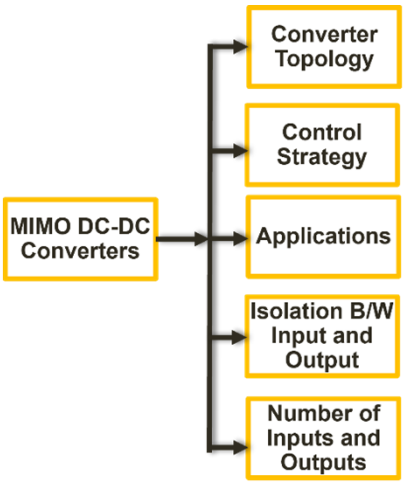

Fig.7. Classification of MIMO DC-DC Converters

c) Control Strategy: Control strategy-based classification of MIMO DC-DC Converters involves using control strategies like pulse-width modulation and phase-shift modulation to regulate the output voltage and current. These converters can achieve high efficiency and accurate regulation by adjusting the switching frequency and duty cycle.

d) Applications: MIMO DC-DC converters can be classified based on their specific applications, such as renewable energy systems, where they interface various energy sources like solar panels, wind turbines, and energy storage systems to the grid or loads. Like Electric Vehicles and data centres, in electric vehicles, MIMO DC-DC converters can manage power flows between multiple sources, such as batteries, fuel cells, and regenerative braking systems. In Data Centers, MIMO converters are employed for efficient power distribution and management in data center environments. converters can improve power distribution and management in aircraft and spacecraft.

e) Isolation between Input and Output: Isolation means there is no direct electrical connection between the input and output circuits, based on classify Isolated and Non-Isolated DC-DC Converters. Isolated MIMO converters have galvanic isolation between their input and output ports. Classification of Isolation b/w Input and Output DC-DC Converters shown in Fig.8. Insolation Provides several benefits, including: Enhanced safety, Noise reduction, Voltage step-up/step-down, Ground potential difference, Isolation transformer. In Non-isolated MIMO converters do not have galvanic isolation between their input and output ports. Instead, they directly transfer power between the input and output circuits. Non-isolated MIMO converters are typically smaller, lighter, and more cost-effective compared to isolated versions. However, they lack the benefits of isolation includes No isolation transformer, Simplicity and cost-effectiveness, Potential for ground loops.

f) Number of Inputs/Outputs: General representation for a converter with N inputs and M outputs (NxM MIMO Converter) Suppose the number of inputs and outputs is increased. In that case, automatically, the network elements will also be increased, and at the same time, the remaining parameters like efficiency, voltage gain, and capacity are also taken into account.

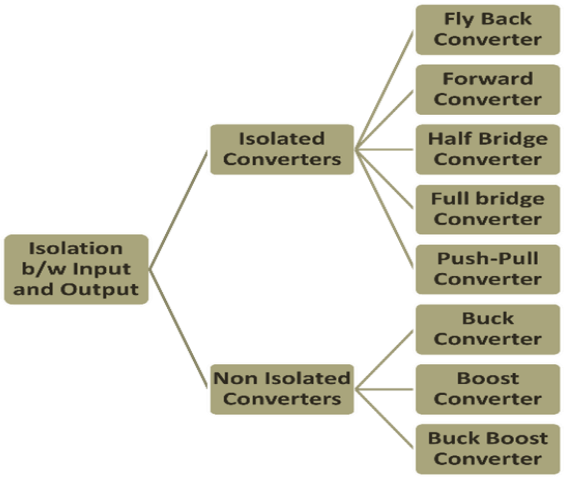

Fig. 8. Classification of Isolation b/w Input and Output DC-DC Converters

B. *Analysis of MIMO DC-DC converters*

Edpuganti etc all [7] proposed various MIMO converter topologies, as illustrated in Fig. 9. One such converter design is for CubeSat EPS, integrating PV panels, batteries, and loads using a single inductor to reduce the converter's size. The outputs are linked in series and connected to loads and the battery through a single inductor. PV panels are connected in parallel to a capacitor and a half-bridge (HB) module, while a full-bridge (FB) module interfaces with the battery. The HB modules regulate voltages for the loads, with outputs from the load-side HB and FB modules connected in series. Power transfer from sources to loads occurs through inductor current. Both the HB and FB modules contain switches that operate in a complementary manner when turned on.

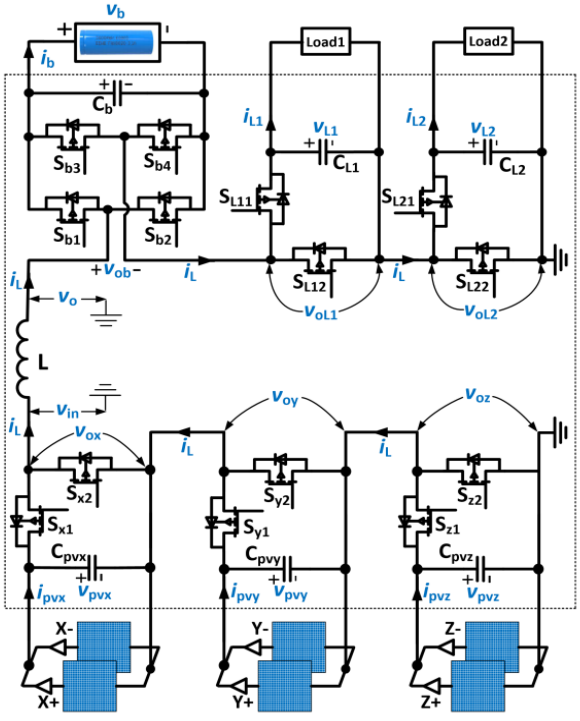

Fig.9 Topology for MIMO converters in CubeSat EPS [7]

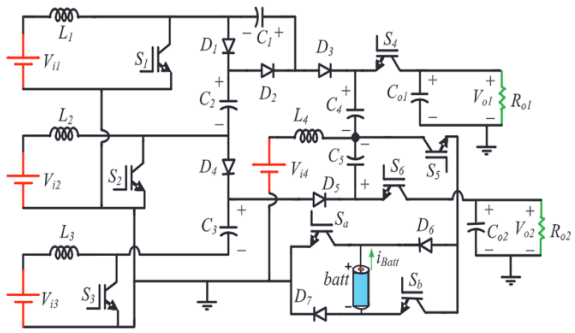

Fig.10. Proposed MIMO converter topology of B-MIMO-C topology [8]

A novel high-step-up bidirectional DC-DC converter with many inputs and outputs is proposed by Mohammad Maalandish etc all [8] shown in Fig.10. The battery represents one of the five inputs of a topology that also features two outputs. Since the transformer is bidirectional, it can bypass, charge, and discharge the battery. Continuous input current, independent input control, and decreased semiconductor normalised voltage stress are advantages. The proposed topology is suitable for electric vehicle applications and has been tested in laboratory for an 870W prototype, confirming theoretical calculations.

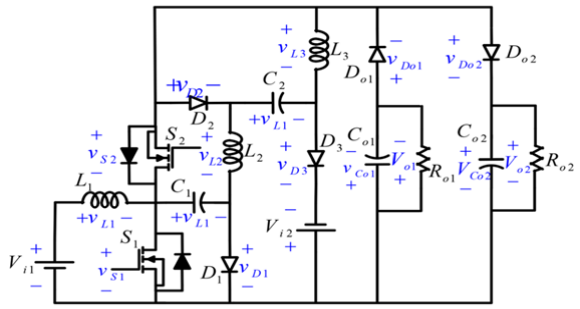

Fig.11. High step-up A non-isolated MIMO DC–DC converter [9]

Saeed Azmoon Asmarood etc all [9] proposed a new High step-up A non-isolated MIMO DC–DC converter shown in Fig.11. It has double-input and double-output ports. The converter is ideal for high step-up clean energy applications, with one output voltage being negative and the other positive. The proposed converter offers several advantages, including higher voltage growth compared to similar converters, lower manufacturing costs, lower conduction and switching losses, and a simpler control method.

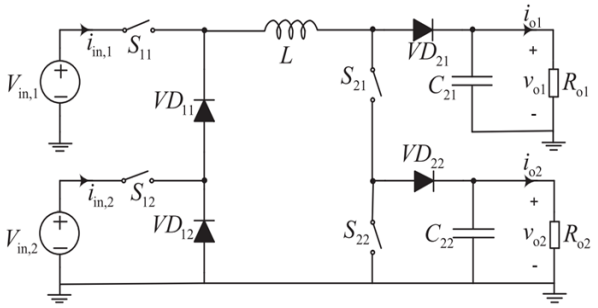

Fig.12 Current-source-mode Single Inductor MIMO converter [10]

Zheng Dong etc all [10] proposed the current-source-mode Single inductor MIMO converter shown in Fig. 12. which avoids cross-regulation and simplifies control strategies. The CSM configuration shares common ground for inputs and outputs, making expansion easier. the development of CSM single-inductor dual-input dual-output (SIDIDO) dc-dc converters has led to a reduction in the number of main circuit components. These converters are capable of working independently even when input sources are disconnected.

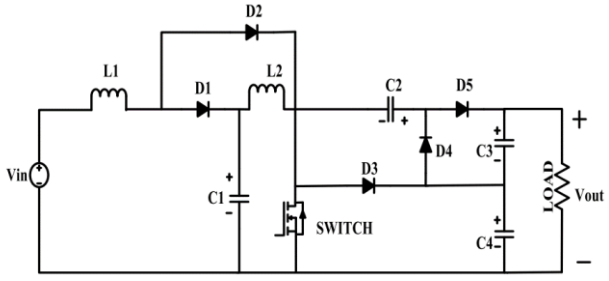

Fig. 13A non-isolated high-gain DC-DC converter topology [11]

Farha Khan etc all [11] Presents better-quality high gain non-isolated quadratic step-up architecture shown in Fig.13. for distribution generation, generating high voltage gain with condensed duty cycles. The proposed topology uses fewer components, reducing the number of inductors and diodes needed. The continuous input current suggestively increases Photovoltaic panel lifespan. Both theoretical and practical results from the converter validate the achievable voltage gain, which has an efficiency of 93.4%. Efficiency can be increased by reducing parasitic resistances and switching loss using more efficient power switches.

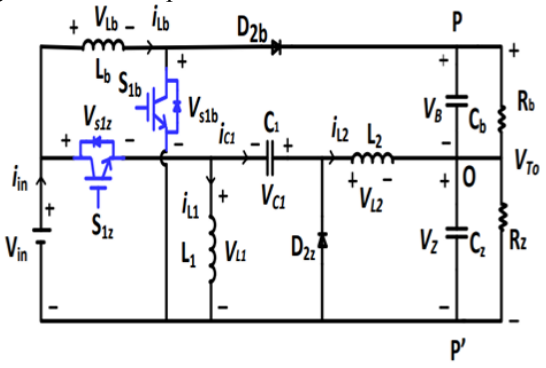

Fig. 14. Proposed interleaved Boost-Zeta converter a monopolar load [12]

Vaishali Chapparya etc all [12] proposed non-isolated Single Input Double Output dc-dc converter, combining Boost and Zeta converter cells with series-connected outputs shown in Fig.14. It can serve as an interface between a renewable energy source and a 48 V BPDC microgrid. The converter has reliable operation, a constant output current, a zero shoot-through possibility, a low current stress, a small number of active components, and a continuous input current. It is efficient and cost-effective. The converter's steady-state and dynamic characteristics were verified through simulation and experimental results. This converter illustrated a 95.61% peak efficiency and a 94.42% average efficiency. Ullah, Q etc all [13] proposed sliding mode control (SMC) based DC–DC Converters for DC Microgrid Applications, shown in Fig. 15, to a step-up the PV system converter, and later extended to include the non-inverting four-switch buck-boost (FSBB) converter network topology for battery and load systems. Parallel to the battery system, the PV system may supply up to 35 V. A FSBB converter allows the DC bus voltage to be adjusted from its current 48 V all the way up to 75 V or all the way down to 5 V. The MATLAB Simulink results demonstrated the robustness and quick dynamic response of the SMC-based FSBB converter during mode shifting, resulting in stable and smooth output waveforms.

Table-1 Work analysis of Non-Isolated and Isolated DC-DC Converters

Ref.	Type of converter	No. of. C and L	No. of. D and S	No. of Windings	Capacity	Effiency (%)
[16]	Non-Isolated	1C,1L	2D,4S	N. A	152W	96.8
[17]	Non-Isolated	1C,2L	2D,4S	N. A	1000W	97
[18]	Non-Isolated	2C,3L	2D,4S	N. A	200W	93.6
[19]	Non-Isolated	3C,2L	0D,4S	N. A	150W	94.11
[20]	Non-Isolated	2C,2L	4D,3S	N. A	300W	96
[21]	Isolated	16C,5L	8D,8S	3	150W	93
[22]	Isolated	2C,1L	8D,4S	3	1000W	91.5
[23]	Isolated	5C,4L	2D,2S	3	500W	94.8
[24]	Isolated	4C,3L	3D,3S	3	250W	95
Capacitors (C), Inductors (L), Diodes (D) and Switches (S); N.A: Not Applicable						

Bharadwaj S. etc all [14] proposed A photovoltaic based Double input double-output (DIDO) DC-DC converter shown in Fig.16. It achieves a conversion efficiency of around 90% in battery charging and discharging modes. This converter improves reliability by utilizing renewable energy sources and reducing control circuit size and complexity. Its on-board battery charging is useful for electric vehicles. By adding input and output ports, the converter topology may support renewable power sources like fuel cells.

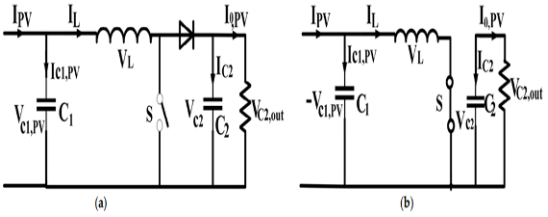

Fig. 15. DC-DC Converters Based on sliding mode control (SMC) Technology (a) during which S is accessible. (b) Timing of the closure of S [13]

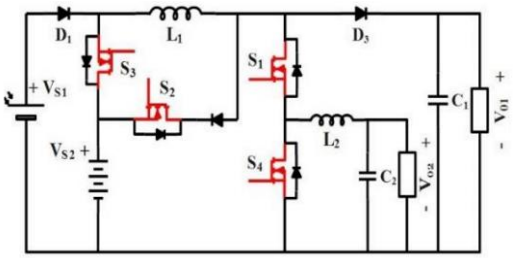

Fig. 16. Proposed double-input doble-output DC-DC converter [14]

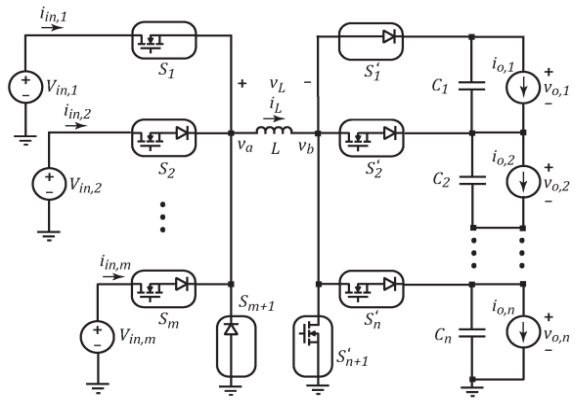

Fig. 17. Proposed MIMO converter with series outputs [15]

Hamid Behjati etc all [15] MIMO DC-DC converters are proposed shown in Fig. 17. This system accommodates multiple input DC sources and passive loads, operates in CCM and DCM, and allows individual regulation of input powers. It uses a single inductor, simplifying current sensing and reducing complexity and cost. It can determine input and output currents without additional circuitry, and output voltages can be higher or lower than the maximum input voltage.

Work analysis was observed for the isolated and non-isolated DC- dc converters shown in Table 1 and also observe the MIMO performance comparison [25,26,27] based on the Controller shown in Fig.18.

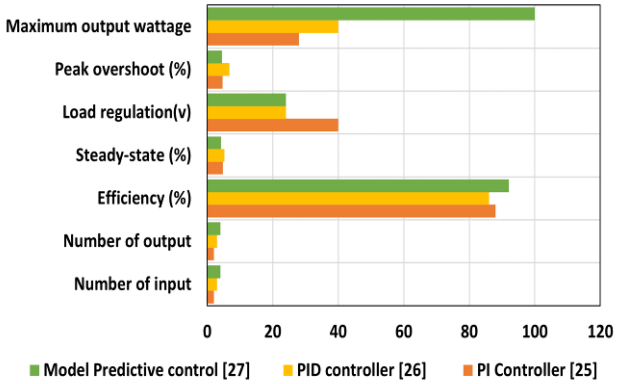

Fig.18. MIMO performance comparison based on the Controller

IV. CONCLUSIONS

Multiple-Input and Multiple-Output DC-DC converters are a promising solution for addressing power distribution and management challenges in DC microgrid systems. They offer improved efficiency and reliability by efficiently redistributing power among multiple input sources and output loads. These converters also enable better integration of renewable energy sources and energy storage devices. The study discussed in the paper provides a comprehensive analysis of MIMO DC-DC converters, focusing on performance metrics, efficiency, and control strategies. The findings contribute to the development of efficient and reliable MIMO DC/DC converters for microgrid (DC) applications.

REFERENCES

[1] Yan, Zhongzhen, Xinyuan Zhu, Yiming Chang, Xianglong Wang, Zhiwei Ye, Zhigang Xu, and Ashk Fars. "Renewable energy effects on energy management based on demand response in microgrids environment." RenewableEnergy (2023).https://doi.org/10.1016/j.renene.2023.05.051

[2] Uddin, Moslem, Huadong Mo, Daoyi Dong, Sondoss Elsawah, Jianguo Zhu, and Josep M. Guerrero. "Microgrids: A review, outstanding issues and future trends." Energy Strategy Reviews 49 (2023): 101127. https://doi.org/10.1016/j.esr.2023.101127

[3] Hernández-Mayoral, Emmanuel, Manuel Madrigal-Martínez, Jesús D. Mina-Antonio, Reynaldo Iracheta-Cortez, Jesús A. Enríquez-Santiago, Omar Rodríguez-Rivera, Gregorio Martínez-Reyes, and Edwin Mendoza-Santos. 2023. "A Comprehensive Review on Power-Quality Issues, Optimization Techniques, and Control Strategies of Microgrid Based on Renewable Energy Sources" Sustainability 15, no. 12: 9847. https://doi.org/10.3390/su15129847

[4] Alam, Md Shafiul, Fahad Saleh Al-Ismail, Syed Masiur Rahman, Md Shafiullah, and Md Alamgir Hossain. "Planning and protection of DC microgrid: A critical review on recent developments." Engineering Science and Technology, an International Journal 41 (2023): 101404. https://doi.org/10.1016/j.jestch.2023.101404

[5] Saikumar Puppala, Devendra Potnuru, Piyush Pratap Singh. Study of Multiple-Input Multiple-Output DC-DC Converter for DC Microgrid Applications. Trends in Electrical Engineering. 2023; 13(3): 16–23 pages. https://doi.org/10.37591/.v13i3.7646

[6] Donthu, Naveen, Satish Kumar, Debmalya Mukherjee, Nitesh Pandey, and Weng Marc Lim. "How to conduct a bibliometric analysis: An overview and guidelines." Journal of business research 133(2021):285296.
https://doi.org/10.1016/j.jbusres.2021.04.070

[7] Edpuganti, Amarendra, Vinod Khadkikar, Naji Al Sayari, and Bashar Zahawi. "Single-Inductor Multiple-Input–Multiple-Output Converter for CubeSats Electric Power System." IEEE Transactions on Power Electronics 38, no. 5 (2023): 6319-6336. https://doi.org/10.1109/TPEL.2023.3243928.

[8] Maalandish, M., Hosseini, S.H., Sabahi, M., Rostami, N., Khooban, M.-H.: B-MIMO high step-up DC/DC converter with high capability to control inputs. IET Power Electron. 16, 1499–1513 (2023). https://doi.org/10.1049/pel2.12486.

[9] Azmoon-Asmarood, S., Maalandish, M., Shoghli, I., Nazemi-Oskuee, S.H.R., Hosseini, S.H.: A non-isolated high step-up MIMO DC-DC converter for renewable energy applications. IET Power Electron. 15, 953–962 (2022). https://doi.org/10.1049/pel2.12281.

[10] Dong, Zheng, Zhen Li, Xiaolu Lucia Li, K. Tse Chi, and Zhenbin Zhang. "Single-inductor multiple-input multiple-output converter with common ground, high scalability, and no cross-regulation." IEEE Transactions on Power Electronics 36, no. 6 (2020): 6750-6760. https://doi.org/10.1109/TPEL.2020.3036704

[11] Khan, Farha, Mohammad Zaid, Abu Tariq, and Mohammad Muktafi Ali Khan. "A new non-isolated high-gain DC-DC converter for the PV application." e-Prime-Advances in Electrical Engineering, Electronics and Energy 5 (2023): 100198. https://doi.org/10.1016/j.prime.2023.100198

[12] Chapparya, Vaishali, Anubrata Dey, and Sajjan Pal Singh. "A Novel Non-isolated Boost-Zeta Interleaved DC-DC Converter for Low Voltage Bipolar DC Micro-grid Application." IEEE Transactions on
Industry Applications (2023).
https://doi.org/10.1109/TIA.2023.3284810

[13] [13]. Ullah, Qudrat, Tiago Davi Curi Busarello, Danilo Iglesias Brandao, and Marcelo Godoy Simões. 2023. "Design and Performance Evaluation of SMC-Based DC–DC Converters for Microgrid Applications" Energies 16, no. 10: 4212. https://doi.org/10.3390/en16104212

[14] Bharadwaj, S., Kr Santha, and S. Arulmozhi. "Design And Analysis Of Integrated Dual-Input Dual-Output DC-DC Converter For Electric Vehicle And Drives Applications." In 2023 9th International Conference on Electrical Energy Systems (ICEES), pp. 681-686. IEEE, 2023. 10.1109/ICEES57979.2023.10110154

[15] Behjati, Hamid, and Ali Davoudi. "A multi-port dc-dc converter with independent outputs for vehicular applications." In 2011 IEEE Vehicle Power and Propulsion Conference, pp. 1-5. IEEE, 2011.10.1109/VPPC.2011.6042983

[16] Varesi, K. , Hosseini, S. H. , Sabahi, M. , Babaei, E., & Vosoughi, N. (2017). Performance and design analysis of an improved non-isolated multiple input buck DC-DC converter. IET Power Electronics, 10(9), 1034-1045. https://doi.org/10.1049/iet-pel.2016.0750.

[17] Akar, F. , Tavlasoglu, Y. , Ugur, E. , Vural, B., & Aksoy, I. (2015). A bidirectional no isolated multi-input DC-DC converter for hybrid energy storage systems in electric vehicles. IEEE Transactions on Vehicular Technology, 65(10), 7944-7955. https://doi.org/10.1109/TVT.2015.2500683.

[18] Chandrasekar, B. , Nallapemmal, C. , Padmanaban, S. , Bhaskar, M. S., Holm-Nielsen, J. B. , Leonowicz, Z., & Masebinu, S. O. (2020). Non-isolated high-gain triple port DC-DC buck-boost converter with ositive output voltage for photovoltaic applications. IEEE Access, 8, 113649-113666. https://doi.org/lo.1109/ACCESS.2020.3003192.

[19] Yi, W. , Ma, H., Peng, S. , Liu, D., Ali, Z. M. , Dampage, U. , & Hajjiah, A. (2022). Analysis and implementation ofmulti-polt bidirectional converter for hybrid energy systems. Energy Reports, 8, 1538-1549. https://doi.org/10.1016/j.egyr.2021.12.068.

[20] .Farakhor, A. , Abapour, M. , & Sabahi, M. (2019). Design, analysis, and implementation of a multiport DC—DC converter for renewable energy applications. IET Power Electronics, 12(3), 465-475. http://dx.doi.org/lO.1049/iet-pel.2018.5633.

[21] Liu, S. , Zhang, X., Guo, H., & Xie, J. (2010, June). Multiput DC/DC Converter for stand-alone photovoltaic lighting system with batte1Y storage. In 2010 International Conference on Electrical and Control Engineering (pp. 3894-3897). IEEE .https://doi.org/lo.1109/iCECE.2010.950.

[22] Wen, H. (2013, June). Determination of the optimal sub-mode for bidirectional dual-active-bridge DC-DC converter with multi-phaseshift control. In 2013 IEEE ECCE Asia Downunder (pp. 596-600). IEEE. https://doi.o@lo.1109/ECCE-Asia.2013.6579159.

[23] Zhu, H. , Zhang, D., Athab, H. S., Wu, B. , & Gu, Y. (2014). PV isolated three-port converter and energy-balancing control method for PVbattery power supply applications. IEEE Transactions on Industrial Electronics, 62(6),3595-3606. https://doi.org/10.1109/TIE.2014.2378752.

[24] Biswas, S., Dhople, S. , & Mohan, N. (2013, November). A three-pon bidirectional dc-dc converter with zero-ripple terminal currents for pv/microgrid applications. In IECON 2013-39th Annual Conference of the IEEE Industrial Electronics Society (pp. 340-345). IEEE .https://doi.org/10.1109ÆECON.2013.6699159.

[25] H. Behjati, A. Davoudi, A multiple-input multiple-output DC-DC converter, IEEE Trans. Ind. Appl. 49 (3) (2013) 1464–1479, https://doi.org/10.1109/ tia.2013.2253440.

[26] X.L. Li, Z. Dong, C.K. Tse, D.D.C. Lu, Single-inductor multi-input multi-output DCDC converter with high flexibility and simple control, Ieee Trans. Power Electron. (2020), https://doi.org/10.1109/tpel.2020.2991353, 1–1.

[27] G. Chen, Y. Liu, X. Qing, M. Ma, Z. Lin, Principle and topology derivation of single inductor multi-input multi-output DC–DC converters, Ieee Trans. Ind. Electron. 68 (January 1) (2021) 25–36, https://doi.org/10.1109/TIE.2020.2965490.

An Integrated Boost Dual Output Series Loaded Resonant Converter for LED Applications with Wide Input Variation

Sree Vidhya Vaidyanadhan
Electrical and Electronics Enginnering
Gayatri Vidya Parishad College of Engineering for Women
Visakhapatnam, India
sri.vydhyanadhan@gvpcew.ac.in

Sankar Peddapati
Electrical Enginnering
National Institute of Technology Andhra Pradesh
Tadepalligudem, India
sankarp@nitandhra.ac.in

Balram kumar
Electrical Enginnering
National Institute of Technology Andhra Pradesh
Tadepalligudem, India
pf052102@student.nitandhra.ac.in

2024 IEEE 4th International Conference on Sustainable Energy and Future Electric Transportation (SEFET) | 979-8-3503-8399-7/24/$31.00 ©2024 IEEE | DOI: 10.1109/SEFET61574.2024.10717999

***Abstract* - This paper proposes a dual output series resonant converter suitable for LED lighting applications, accommodating wide input voltage variations. It utilizes a five-switch converter configuration integrated with boost converter for powering two light emitting diode (LED) lamps. An asymmetric voltage cancellation (AVC) is used for independent current control integrating dimming feature. The paper presents detailed circuit operation, and steady state analysis with simulation results validating performance of dual 36W LED loads (i.e. total output power of 72 W). Comparative study highlights advantages over existing LED driver designs.**

Keywords— ***Boost integrated series loaded resonant converter, dual-output, soft-switching, asymmetrical voltage control, wide input variation, LED driver.***

I.INTRODUCTION

LED lighting has revolutionized global lighting systems such as indoor and outdoor lighting, automotive lighting, and advertising [1-2] with its improved efficiency and easy dimming capabilities, significantly enhancing lighting quality while reducing energy consumption and maintenance costs. Precise current control is essential due to the exponential V-I characteristic of LEDs, necessitating to the use of switched-mode power converter [3-4]. AC-DC converters are employed to power LEDs from AC sources, often incorporating power factor correction while minimizing or eliminating electrolytic capacitors due to their short lifespan [5-8]. Multi-output converters with fewer components are preferred for applications with multiple loads, offering high power density and improved efficiency. Resonant converter topologies like series, parallel, series-parallel, etc are integrated to achieve zero voltage switching (ZVS) or zero current switching (ZCS). In automotive lighting applications, LED drivers must accommodate wide variations in battery voltage during transient conditions like starting, acceleration, and braking. Multiple outputs are required for various lighting functions such as main head lamps, tail lamps, brake lamps, and side lamps, each with equal or different voltage and wattage requirements. Configurations are proposed to address these challenges and ensure effective LED current control under varying conditions.

In [9], full-bridge configuration efficiently handles multiple-loads with fewer components and reduced conduction losses but lacks independent dimming control. Multiple output LED drivers presented in [10-11] employs asymmetric duty cycle control with soft switching but has limited voltage gain. In [12], a full-bridge configuration achieves high efficiency with soft switching but not ideal for automotive applications due to significant source variations. In [13-14], half and full-bridge configurations integrate buck-boost operation. They feature a reconfigurable design to manage wide input variations efficiently. However, they utilize variable frequency control for the buck-boost configuration.

This paper introduces an LED driver configuration for automobile applications featuring two LED loads. Utilizing a five-switch setup with a series LC circuit as the power processing unit, it enables independent control of both loads.

II. CIRCUIT DESCRIPTION

A five-switch configuration is proposed to power two LED loads with independent control as shown in Fig.1. It provides independent control of both loads. It uses series resonant circuit to achieve zero voltage switching (ZVS) of the converter devices. This configuration is used for applications with wide input voltage variations such as automobile lighting, etc. The first leg of the converter consists of switches S_1 and S_2, each operated with 50% duty cycle. The second leg incorporates switches S_3, S_4 and S_5, with controllable gating pulses of S_3 and S_5. The gate pulse of S_4 is derived from the gating signals of S_3 and S_5. The tank voltages V_{AB} and V_{AC}, are independently controlled using asymmetrical voltage cancellation (AVC) technique to drive current through the corresponding resonant circuits. Diode bridge rectifiers (D_{11}-D_{14}) and (D_{21}-D_{24}), are utilized to rectify resonant currents (i_{r1} and i_{r2}) and filtered by capacitors (C_{o1} and C_{o2}), and thus flow. through LED load. Dimming control for the LED loads is facilitated by switches S_{D1} and S_{D2}. To address wide input voltage variations, a boost circuit is integrated with the five-switch configuration. Switches S_1 and S_2 also serve as part of boost configuration, operating with a 50% duty cycle. Consequently, the DC bus voltage across C_{Boost}, is double that of battery voltage ranging from 40 V to 64 V to accommodate input voltage variations from 20 V to 32 V.

A. Principle of Operation

The proposed configuration independently powers two LED loads, achieving current regulation is achieved through AVC control of V_{AB} and V_{AC} as shown in Fig.2. Soft-switching is enabled by a series resonant circuit, with a ratio of switching frequency(ω_s) to resonant frequency (ω_r), set as $\omega_s / \omega_r = 1.1$ to achieve ZVS operation. Gate pulses for all the devices ($V_{g1} - V_{g5}$), tank input voltages V_{AB} and V_{AC}, and tank currents i_{r1} and i_{r2} are illustrated Fig. 2. Dimming of LED lamps, is accomplished by switches S_{D1} and S_{D2} connected in series with their respective resonant tank circuits. Turning off the dimming switches results in the lamps being off, while

turning them on controls LED current to remain constant, allowing for varying levels of illumination by adjusting the duty cycle of dimming switches.

Fig.1 depicts the closed loop operation of the proposed converter used for the generation of gating pulses. Gating pulses, V_{g1} and V_{g2} operate at 50% duty ratio. Two control voltages, V_{c1} and V_{c2} are compared with the sawtooth waveform, with frequency twice that of operating frequency. This yields control pulses V_{c1} and V_{c2} as shown in Fig.2. These control pulses are ANDed with V_{g1} and V_{g2} respectively. Incorporating dead-time, t_d and OR-ing these signals results in V_{g4}. Additionally, the complementary signals of [V_{c1} AND V_{g1}] and [V_{c2} AND V_{g2}] yield V_{g3} and V_{g5}, respectively. Different voltage levels of V_{AB} and V_{AC} such as $+V_{DC}$, zero and $-V_{DC}$ are generated as follows.

The voltages, V_{AB} and V_{AC} will have voltage level of -

(i)$+V_{DC}$ when S_1, S_4 and S_5 are ON,

(ii)$-V_{DC}$ when S_2, S_3 and S_4 are ON, and

(iii)zero when both S_1 and S_3 are ON or S_2 and S_5 are ON respectively.

Tank voltages, V_{AB} and V_{AC} drive sinusoidal currents i_{r1} and i_{r2}, in the resonant tank. These currents are rectified and filtered by output capacitors C_{o1} and C_{o2}. LED load currents are kept constant despite supply voltage variations through AVC control of V_{AB} and V_{AC}. Integration of the boost configuration with switches S_1 and S_2 aids in regulating load current against wide battery voltage fluctuations. The converter's performance is evaluated through MATLAB simulations.

B. Modes of operation

Mode-I (t_0-t_1): In this mode, at $t = t_0$, S_2 and S_3 are turned-OFF, while S_5 remain ON. When S_2 is switched off, the boost inductor current, i_{LB} reaches its peak and remains constant from t_0 to t_1. During this interval, tank currents i_{r1} and i_{r2} are negative. In this mode, tank current ($i_{r1}/2$), charges C_{s3} and discharges C_{s4}, while the current ($i_{r1}+i_{r2}+i_{LB}$)/2, charges C_{s2} and discharges C_{s1}. Additionally, V_{AB} changes from $-V_{DC}$ to $+V_{DC}$, V_{AC} changes from zero to $+V_{DC}$ as shown in Fig.3 (a).

$$
\begin{aligned}
&i_{s1} = i_{s2} = i_{S3} = i_{S4} = 0 \\
&i_{s5} = [\frac{(i_{r1})}{2} + (i_{r2})] \\
&v_{LB} = V_{in}
\end{aligned}
\tag{1}
$$

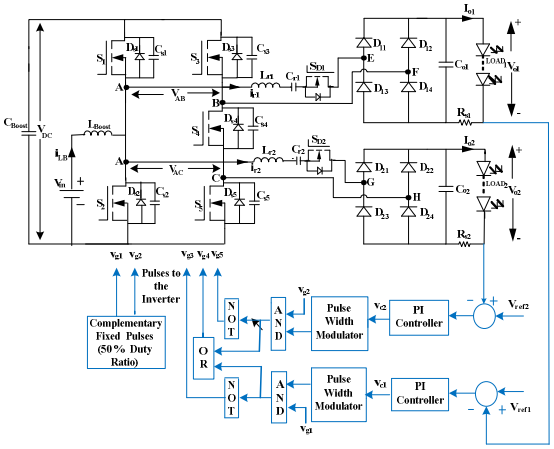

Fig. 1 Circuit diagram of proposed converter

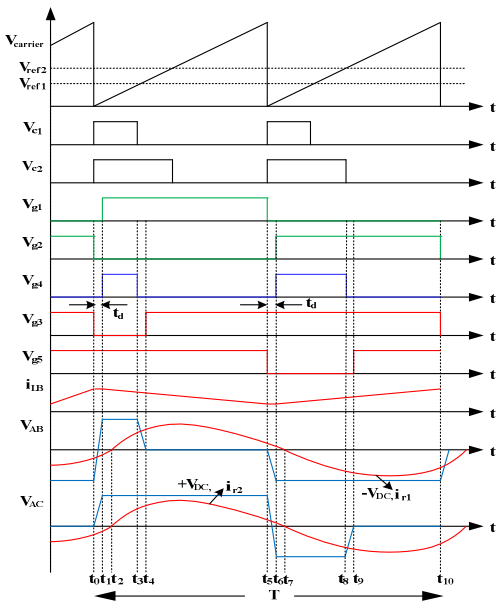

Fig.2 Operational waveforms of the converter

Mode-2 (t_1-t_2): At $t = t_1$, S_1 and S_4 are triggered for ZVS turn-ON while S_5 remain ON as shown in Fig.3 (b). Boost inductor current, i_{LB} decreases linearly transferring energy to boost capacitor, C_{Boost}. In this mode, the tank currents i_{r1} and i_{r2} remain negative with V_{AB} and V_{AC} at $+V_{DC}$. By $t = t_2$, i_{r1} and i_{r2} reach zero, the voltages across C_{s2} and C_{s3} becomes $+V_{DC}$ and C_{s1} and C_{s4} become zero.

$$
\begin{aligned}
&i_{s1} = -(i_{r1} + i_{r2} + i_{LB}) \\
&i_{s2} = i_{s3} = 0 \\
&i_{s4} = -i_{r1} \\
&i_{s5} = -(i_{r1} + i_{r2}) \\
&v_{LB} = (V_{DC} - V_{in})
\end{aligned}
\tag{2}
$$

Mode-3 ($t_2 - t_3$): During this mode, switches S_1, S_4 and S_5 remain ON as shown in Fig. 3 (c). Tank voltages V_{AB} and V_{AC} are at $+V_{DC}$. Tank currents i_{r1} and i_{r2} start increasing from zero to positive. Boost inductor current, i_{LB} linearly decreases, transferring energy from L_{Boost} to C_{Boost}. At $t=t_3$, i_{r1} reaches its peak while i_{r2} continues to rise beyond t_3 as V_{AC} has higher duty cycle than V_{AB}.

$$
\begin{aligned}
&i_{s1} = (i_{r1} + i_{r2} - i_{LB}) \\
&i_{s2} = i_{s3} = 0 \\
&i_{s4} = i_{r1} \\
&i_{s5} = (i_{r1} + i_{r2}) \\
&v_{LB} = (V_{DC} - V_{in})
\end{aligned}
\tag{3}
$$

Mode-4 (t_3-t_4): At $t=t_3$, S_4 switches OFF with ZVS, while S_1 and S_5 remain ON and S_2 and S_3 remain OFF. Tank currents, i_{r1} and i_{r2} become positive as shown in Fig.3 (d). Inductor current, i_{LB} linearly decreases. During this mode, V_{AB} transitions from $+V_{DC}$ to zero, while V_{AC} stays at $+V_{DC}$. Half of i_{r1} discharges the snubber capacitors C_{s3} from $+V_{DC}$ to zero, and the other half charges C_{s4} zero to V_{DC}. i_{r2} flows from the source through S_1, load-2, S_5 and back to the source. At $t = t_4$, S_3 turns ON with ZVS.

$$
\begin{aligned}
&i_{s1} = (i_{r1} + i_{r2} - i_{LB}) \\
&i_{s2} = i_{s3} = i_{s4} = 0
\end{aligned}
$$

$$i_{s5} = \left(\frac{i_{r1}}{2} + i_{r2}\right)$$
$$v_{LB} = (V_{DC} - V_{in}) \quad (4)$$

Mode-5 (t_4-t_5): At t=t_4, S_3 switches ON with ZVS. During this interval, S_1, S_3 and S_5 are ON and S_2 and S_4 are OFF as depicted in Fig. 3 (e). Hence, $V_{AB} = 0$ and $V_{AC} = +V_{DC}$. Tank currents, i_{r1} and i_{r2} are positive.

$$i_{s1} = (i_{r1} + i_{r2} - i_{LB})$$
$$i_{s2} = i_{s4} = 0$$
$$i_{s3} = -i_{r1}$$
$$i_{s5} = i_{r2}$$
$$v_{LB} = (V_{DC} - V_{in}) \quad (5)$$

Mode-6 (t_5-t_6): At t=t_5, S_1 and S_5 are turned-OFF. In this mode, boost inductor current, i_{LB} reaches its minimum and remain constant. The tank currents i_{r1} and i_{r2} are positive, half of i_{r2} flowing through S_5, charges C_{S5} and discharges C_{s4} as shown in Fig.3 (f). Similarly, the current $(i_{r1}+i_{r2}-i_{LB})/2$, charges C_{s1} and discharges C_{s2}. V_{AB} transitions from zero to $-V_{DC}$, and V_{AC} shifts from $+V_{DC}$ to $-V_{DC}$. At t=t_6, C_{s1} and C_{s5} charge to V_{DC} and C_{s2} and C_{s4} discharge to zero, resulting in V_{AB} and V_{AC} becomes equal to $-V_{DC}$.

$$i_{s1} = i_{s2} = i_{s4} = i_{S5} = 0$$
$$i_{s3} = -\left[(i_{r1}) + \frac{(i_{r2})}{2}\right]$$
$$v_{LB} = (V_{DC} - V_{in}) \quad (6)$$

Mode-7 (t_6-t_7): At t = t_6, in Fig. 3 (g), S_2 and S_4 turn- ON with ZVS, while S_3 remains ON. During this interval, boost inductor current, i_{LB} increases linearly. Tank currents i_{r1} and i_{r2} are positive and reach zero at t = t_7. In this mode, $V_{AB} = V_{AC} = -V_{DC}$.

$$i_{s1} = i_{s5} = 0$$
$$i_{s2} = (i_{LB} - i_{r1} - i_{r2})$$
$$i_{s3} = -(i_{r1} + i_{r2})$$
$$i_{s4} = -i_{r2}$$
$$v_{LB} = (V_{DC} - V_{in}) \quad (7)$$

Mode-8 (t_7-t_8): During this mode, depicted in Fig. 3 (h), switches S_2, S_3 and S_4 remain ON. Tank voltages V_{AB} and V_{AC} are equal to $-V_{DC}$, with negative tank currents i_{r1} and i_{r2}. Boost inductor current, i_{LB} increases linearly. At t=t_8, i_{r2} reaches its peak while i_{r1} continues rising due to V_{AB} having higher duty cycle than V_{AC}.

$$i_{s1} = i_{s5} = 0$$
$$i_{s2} = (i_{r1} + i_{r2} + i_{LB})$$
$$i_{s3} = (i_{r1} + i_{r2})$$
$$i_{s4} = i_{r2}$$
$$v_{LB} = V_{in} \quad (8)$$

Mode-9 (t_8-t_9): At t=t_8, S_4 turns OFF with ZVS, while S_2 and S_3 remain ON and S_1 and S_5 remain OFF. Tank currents i_{r1} and i_{r2} are negative. Boost inductor current, i_{LB} continues to increase linearly. During this mode, V_{AB} stay at $-V_{DC}$ while V_{AC} changes from $-V_{DC}$ to zero. Half of i_{r2} discharges C_{s5} from V_{DC} to zero, and the other half charges C_{s4} from zero to V_{DC} as shown in Fig. 3 (i). At t = t_9, S_5 is turned ON with ZVS.

$$i_{s1} = i_{s5} = i_{s4} = 0$$
$$i_{s2} = (i_{r1} + i_{r2} + i_{LB})$$
$$i_{s3} = \left(i_{r1} + \frac{i_{r2}}{2}\right)$$
$$v_{LB} = V_{in} \quad (9)$$

Mode-10 (t_9-t_{10}): At t=t_9, S_5 turns ON with ZVS. During this interval, S_2, S_3 and S_5 are ON while S_1 and S_4 are OFF as is shown in Fig. 3 (j). Thus, $V_{AB} = -V_{DC}$ and $V_{AC} = 0$. Tank currents, i_{r1} and i_{r2} are negative.

$$i_{s1} = i_{s4} = 0$$
$$i_{s2} = (i_{r1} + i_{r2} + i_{LB})$$
$$i_{s3} = i_{r1}$$
$$i_{s5} = i_{r2}$$
$$v_{LB} = V_{in} \quad (10)$$

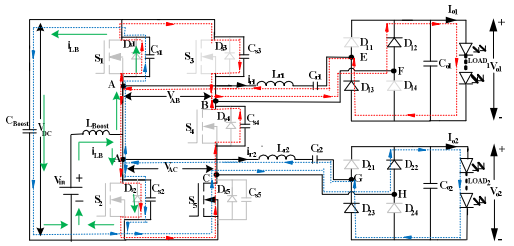
(a)

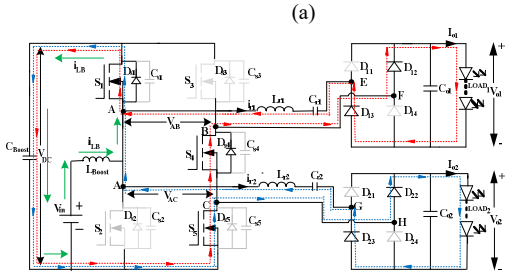
(b)

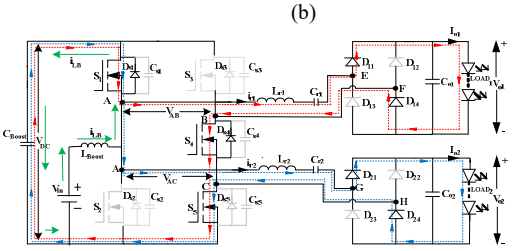
(c)

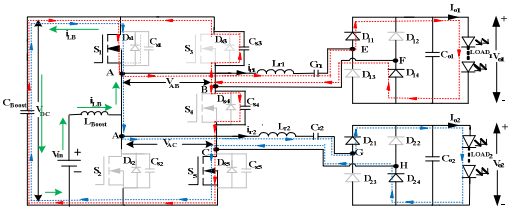
(d)

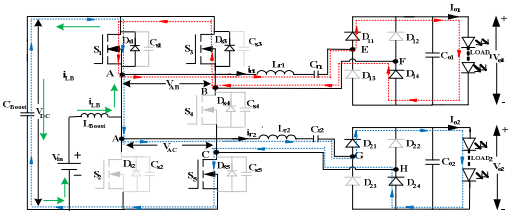
(e)

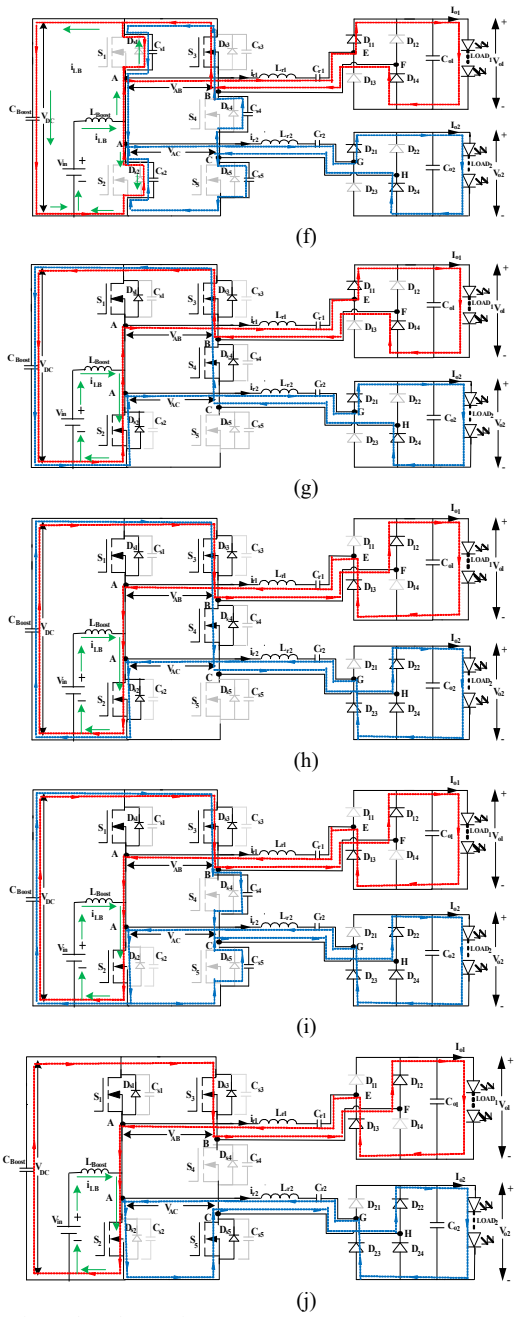

Fig.3 (a)-(j) Modes of operation

III.RESULTS AND DISCUSSIONS

A. Simulation Results and Discussions

The specifications of the converters used in simulation is shown in Table I and the respective results depict the operation of the proposed converter for a battery voltage of 24V, showcasing various waveforms in Fig. 4 (a) and (b) These figures, illustrate battery voltage (V_{in}), DC link Voltage (V_{DC}), boost inductor voltage and current (V_{LB}, i_{LB}), resonant tank voltages and currents (V_{AB} and i_{r1}) and (V_{AC} and i_{r2}), load Voltages (V_{o1}, V_{o2}), load currents (I_{o1}, I_{o2}), switch voltages and currents (v_{sw1}, i_{sw1}) to (v_{sw5}, i_{sw5}) for 40% dimming of load-1 and 20% dimming of load-2. Load currents are regulated to 1 A under closed-loop operation.

It can be observed that when dimming occurs by opening the series switches of the resonant tanks, the power transfer

Table I. Design parameters of the proposed converter

Parameter	Description
Input Voltage	20V – 32V
Boost inductance, (L_{Boost})	100µH
Boost Capacitor, (C_{Boost})	20 µF
Resonant tanks inductor (L_{r1}, L_{r2}), Resonant tank capacitors (C_{r1}, C_{r2})	51.6 µH, 60.6 nF
Output Voltage of load -1 and load-2	36V (equal)
Output Current of load -1 and load-2	1 A
Switching frequency (f_s)	100kHz
No. of strings, No. of LEDs per string	2, 11
Forward drop of each LED	2.3 V
Forward resistance of each LED	1.9 ohms
Dimming Frequency	100 Hz
LED Current per string of both loads	500mA
PI Controller Parameters, Kp and Ki	0.2, 1000

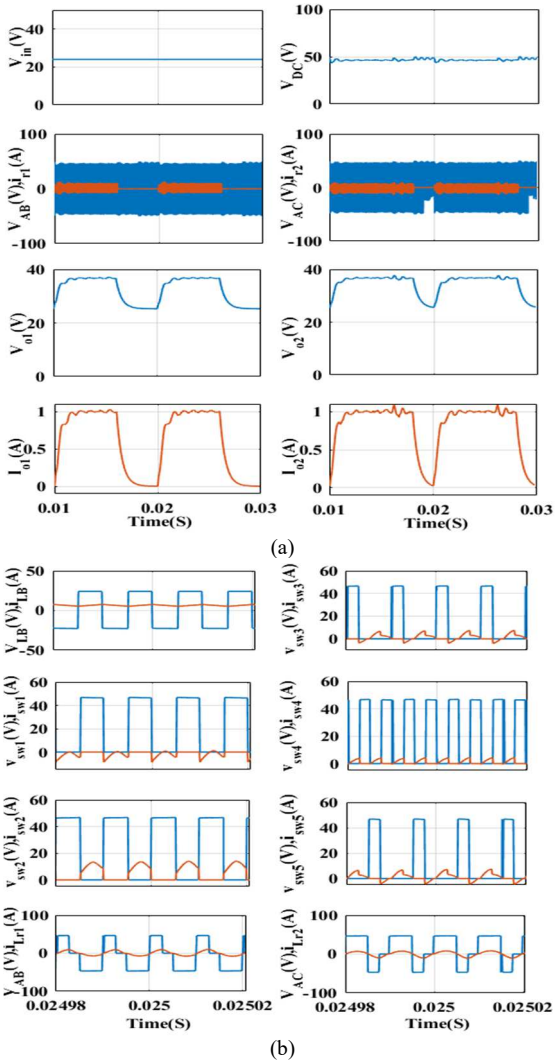

(a)

(b)

Fig. 4 (a) – (b) Simulation waveforms of the converter.

to output is stopped causing output voltages (V_{o1} and V_{o2}) to decrease and LED currents (I_{o1} and I_{o2}) to drop to zero. Upon turning on, LED currents resume to their normal value without overshoot, with corresponding tank currents also becoming zero during these intervals. As depicted in Fig.4 (a) for input voltage of 24 V. Additionally, boost inductor waveforms, and also resonant tanks and devices voltage and current waveforms are depicted to indicate their ZVS/ZCS operation are shown in Fig. 4 (b).

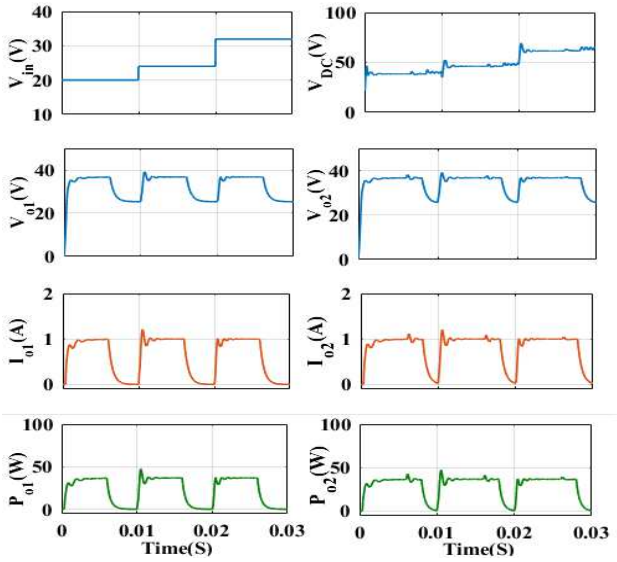

Fig. 5 Step response and its output waveforms

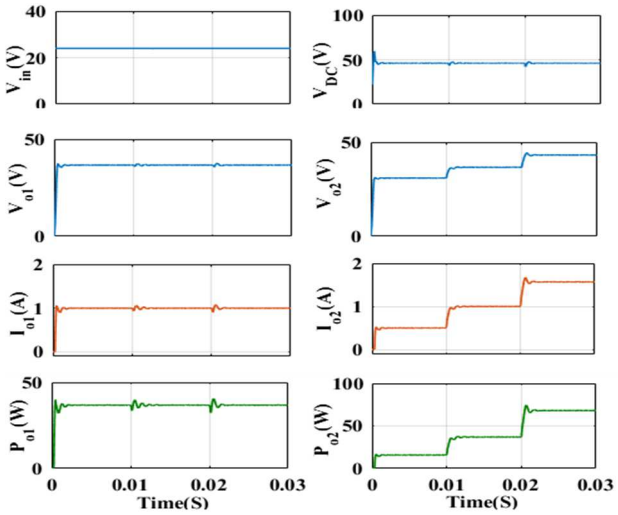

Fig. 6 Independent control of both loads.

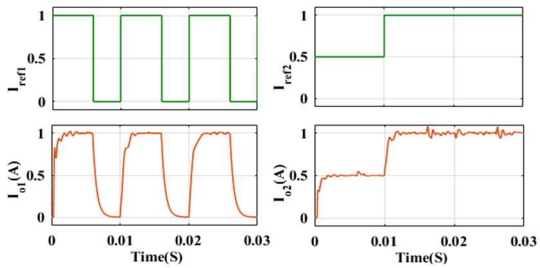

Fig. 7 Dynamic response of load current.

The step response of the proposed converter in closed-loop performed and its output responses (i.e. Vo1, Vo2, Io1, Io2, Po1 and Po2) under dimming conditions, are shown in Fig. 5. It can be seen that output voltages and LED currents are regulated to be constant under variations of the input/battery voltage. Hence, it can be observed that output voltages and LED currents are regulated independently. Independent control operation of the two loads is demonstrated in Fig. 6 for the input voltage of 24V. Here, the reference signal of load-1 is to be constant at 1 A and by changing that of load-2 from 0.5 A to 1 A and then to1.5 A. It can be observed that load-1 current remains constant but only that of load-2 current, voltage, and power are changed. The dynamic response of load-2 w.r.t step change in I_{ref2} is shown in Fig.7 while load-1is operated under dimming condition. The step response is close to first order system.

B. Comparative Analysis

The comparative analysis of existing multiple output dual output is discussed in Table- II. The topologies in [9] and [10] offer independent current control for multiple LED loads, having a higher component count than the proposed LED driver. Conversely, the converter in [11] has fewer components and enables independent operation, but its half-bridge configuration limits voltage gain and results in reduced efficiency due to non-uniform diode-conduction losses. The efficiency of the proposed converter is similar to the existing works. Notably, the converters discussed in [9], [12], [14] and [15] lack independent load regulation operation

Table II Comparison of proposed configuration with existing non-isolated topologies

Features	**[9]**	**[10]**	**[11]**	**[12]**	**[13]**	**[14]**	**[15]**	**Proposed**
No. of switches	2+N	2(1+N)	1+N	N+2	1+2N	2(2N)	2N	2N+1
No. of inductors	3N/2	1+N	N	N+2	1+N	N+1	N	N+1
No. of capacitors	1	2N	2(N+1)	N/3	1+2N	2N+1	N+1	2N+1
No. of diodes	1	4N	4N	2N/3	4N	4N	0	4N
No. of loads (N)	4	2	2	3	2	1	4	2
Components count per load	low	moderate	low	moderate	high	low	moderate	low
Input Voltage (V)	48	48	48	40-60	48	18-120	8-18	20-32
Output Voltage (V)	33 (equal)	42.25, 19.5	16.25, 13	13.68,20.52, 20.52	22.5, 39.6	22.5	3-50	36 (equal)
Peak efficiency (%)	94.96	92.45	91.5	96.1	92.3	94	92.1	93.1
ZVS turn-on	yes	yes	yes	yes	yes	yes	yes	yes
Non-isolated structure	yes	yes	yes	yes	yes	yes	yes	yes
Control complexity	simple	moderate	simple	simple	complex	simple	moderate	simple

to accommodate wide input variations. In [13], frequency control is utilized to maintain a steady output voltage despite variations in the input voltage.

IV.CONCLUSION

An LED driver with wide input variation is presented for two LED lamps suitable for automobile application. Power conversion with series resonant converter is implemented. A boost converter is integrated on source side along with five-switch series resonant converter configuration with wide input variations. For the given battery voltage, boost converter steps up the input voltage and, five-switch resonant converter steps down the output voltage to desired values so that LED load current can be controlled to be constant.

ZVS operation of the devices results in negligible switching losses with improved efficiency. Independent control of each load and dimming are achieved. This configuration is also suitable for handling larger powers. Results are presented for 20 V to 32 V input voltage and 36 V, 1 A current for each load with 36 W of individual load power.

REFERENCES

[1] Y. Wang, J. M. Alonso and X. Ruan, "A Review of LED Drivers and Related Technologies," in IEEE Transactions on Industrial Electronics, vol. 64, no. 7, pp. 5754-5765, July 2017, doi: 10.1109/TIE.2017.2677335.

[2] S. Li, S. -C. Tan, C. K. Lee, E. Waffenschmidt, S. Y. Hui and C. K. Tse, "A survey, classification, and critical review of light-emitting diode drivers," in IEEE Transactions on Power Electronics, vol. 31, no. 2, pp. 1503-1516, Feb. 2016, doi: 10.1109/TPEL.2015.2417563.

[3] M. Esteki, S. A. Khajehoddin, A. Safaee and Y. Li, "LED Systems Applications and LED Driver Topologies: A Review," in IEEE Access, vol. 11, pp. 38324-38358, 2023, doi: 10.1109/ACCESS.2023.3267673.

[4] F. Bento and A. J. M. Cardoso, "Comprehensive survey and critical evaluation of the performance of state-of-the-art LED drivers for lighting systems," in Chinese Journal of Electrical Engineering, vol. 7, no. 2, pp. 21-36, June 2021, doi: 10.23919/CJEE.2021.000013.

[5] A. Pollock, H. Pollock and C. Pollock, "High Efficiency LED Power Supply," in IEEE Journal of Emerging and Selected Topics in Power Electronics, vol. 3, no. 3, pp. 617-623, Sept. 2015, doi: 10.1109/JESTPE.2015.2430621.

[6] Y. Wang, J. Huang, W. Wang and D. Xu, "A Single-Stage Single-Switch LED Driver Based on Class-E Converter," in IEEE Transactions on Industry Applications, vol. 52, no. 3, pp.2618-2626,May-June2016,doi: 10.1109/TIA.2016.2519324.

[7] Ramakrishna Reddy Ch K, Porpandiselvi S, Vishwanathan N. An efficient full-bridge resonant converter for light emitting diode (LED) application with simple current control. Int J Circ Theor Appl. 2019;1–13.

[8] Y. Guo, S. Li, A. T. L. Lee, S. -C. Tan, C. K. Lee and S. Y. R. Hui, "Single-Stage AC/DC Single-Inductor Multiple-Output LED Drivers," in IEEE Transactions on Power Electronics, vol. 31, no. 8, pp. 5837-5850, Aug. 2016, doi: 10.1109/TPEL.2015.2496247.

[9] C. Kasi Ramakrishna Reddy, S. Porpandiselvi, and N. Vishwanathan, "Soft switched full-bridge light emitting diode driver configuration for street lighting application," IET Power Electronics, vol. 11, DOI 10.1049/iet pel.2017.0021, no. 1, pp. 149–159, 2018.

[10] Ch KR, Porpandiselvi S, Vishwanathan N. A three-leg resonant converter for two output LED lighting application with independent control. Int J Circ Theor Appl. 2019;1–15. https://doi.org/ 10.1002/cta.2632.

[11] H. R. Kolla, N. Vishwanathan and B. K. Murthy, "Independently Controllable Dual-Output Half-Bridge Series Resonant Converter for LED Driver Application," in IEEE Journal of Emerging and Selected Topics in Power Electronics, vol. 10, no. 2, pp. 2178-2189, April 2022, doi: 10.1109/JESTPE.2021.3120879.

[12] A. Patakamoori, R. R. Udumula, T. K. Nizami and K. R. R. Ch, "An Efficient Soft-Switched LED Driver for Street Lighting Applications With Input Regulation," in IEEE Journal of Emerging and Selected Topics in Power Electronics, vol. 11, no. 5, pp. 5018-5028, Oct. 2023, doi: 10.1109/JESTPE.2023.3298030.

[13] Veeramallu VKS, SP, BLN., "A buck-boost integrated high gain non-isolated half-bridge series resonant converter for solar PV/battery fed multiple load LED lighting applications". Int J Circ Theor Appl. 2019;1-20. https://doi.org/10.1002/cta.2720.

[14] V. K. S. Veeramallu, S. Porpandiselvi and B. L. Narasimharaju, "A Non-isolated Wide Input Series Resonant Converter for Automotive LED Lighting System," in IEEE Transactions on Power Electronics, vol. 36, no. 5, pp. 5686-5699, May 2021, doi: 10.1109/TPEL.2020.3032159.

[15] S. Mukherjee, V. Yousefzadeh, A. Sepahvand, M. Doshi and D. Maksimović, "A Two-Stage Automotive LED Driver With Multiple Outputs," in IEEE Transactions on Power Electronics, vol. 36, no. 12, pp. 14175-14186, Dec. 2021, doi: 10.1109/TPEL.2021.3077528.

Conference Proceedings
International Conference on Emerging Advances and Applications in Green Energy (ICEAAGE-2024)
Organized by Department of Electrical & Electronics Engineering on 29th February 2024
Prasad V. Potluri Siddhartha Institute of Technology, Kanuru, Vijayawada, Andhra Pradesh, India.

Design of Driver for 50W Light Emitting Diode (LED) lamp

Krishna Perumallapalli, Devendra Potnuru
Rajiv Gandhi University of Knowledge Technologies Nuzvid, India
pkrishnaeee@gmail.com; devendra.p@gvpcew.ac.in

ABSTRACT

This paper presents the comprehensive design and optimization of a 50W Light Emitting Diode (LED) lamp, aimed at achieving superior performance in terms of energy efficiency, luminous efficacy, and thermal management. The growing demand for energy-efficient lighting solutions has fuelled the need for innovative designs in LED lamps, with a focus on maximizing brightness while minimizing power consumption. LED drivers play a critical role in providing the required electrical power to LEDs while addressing various challenges such as power factor correction, thermal management, and flicker reduction. The design process begins with a thorough analysis of the electrical characteristics of the LEDs, considering factors such as forward voltage, forward current, and temperature dependencies. The driver circuit is then tailored to deliver a stable and regulated current, ensuring optimal power utilization and longevity of the LED components. To enhance energy efficiency, power factor correction (PFC) techniques are incorporated, minimizing reactive power and aligning current and voltage waveforms. The designed driver undergoes rigorous testing to evaluate its performance under different operating conditions, including assessments of power factor, total harmonic distortion, and thermal stability. Results demonstrate the effectiveness of the driver in providing a reliable and efficient power supply to the 50W LED lamp. The optimized driver presented in this study not only ensures the reliable operation of a 50W LED lamp but also serves as a scalable model for driving LEDs in various lighting applications, paving the way for advancements in energy-efficient and sustainable lighting technologies. The designed driver simulated using MATLAB and the results are analysed for further improvement of performance.

Keyword: - *LED, LED Driver, Power factor, PFC and MATLAB.*

1 INTRODUCTION

With the ever-increasing demand for energy-efficient and environmentally sustainable lighting solutions, Light Emitting Diode (LED) technology has emerged as a frontrunner in the illumination industry (Uddin et al., 2011). LED lamps offer numerous advantages, including long lifespans, low energy consumption, and superior light quality. However, the efficient operation of LED systems relies heavily on the accompanying driver circuits, which play a pivotal role in regulating the electrical power supplied to the LEDs (Wang et al., 2017). The challenges in designing a driver for a 50W LED lamp are multifaceted. Efficient power management, power factor correction, thermal considerations, and compatibility with smart lighting controls are among the key aspects that demand careful attention (Ali et al.,2016). As the global transition towards energy-efficient lighting intensifies, there is a growing need for advanced driver technologies that not only provide a stable power supply but also offer intelligent features to enhance user experience and adaptability. The basic structures of LED drivers available in the literature are shown in Figure 1 as reported by Wang et al., 2017.

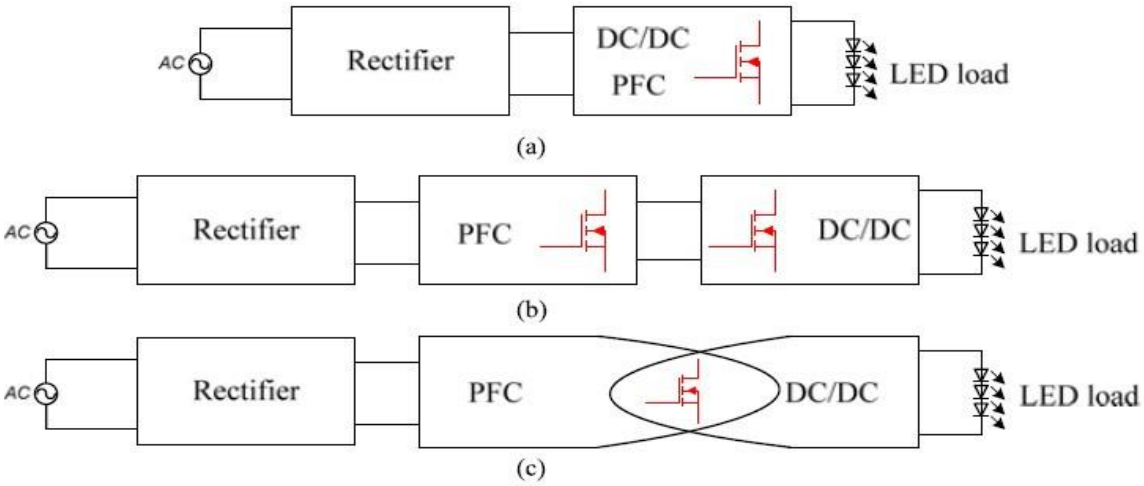

Figure 1: Structure of LED drivers (a) Single stage (b) Two stage (c) Integrated stage

LED drivers serve as the backbone of LED lighting systems, converting incoming electrical power to a form suitable for the LEDs, addressing power quality issues, and ensuring optimal performance (Wang et al., 2017). The design of an effective LED driver is paramount in achieving energy efficiency, longevity of LED components, and compliance with stringent lighting standards. As the available source at the distribution system is AC, there is a need for AC-DC converter (Kim et al., 2017) and DC-DC converter. Various topologies and control schemes of DC-DC converters are available in the literature (P and Potnuru, 2023; Luz et al.,2015; P.Krishna, 2023). The basic DC-DC converters are reviewed and reported by P and Potnuru, 2023 and Wang et al., 2017 and are shown in Figure 2.

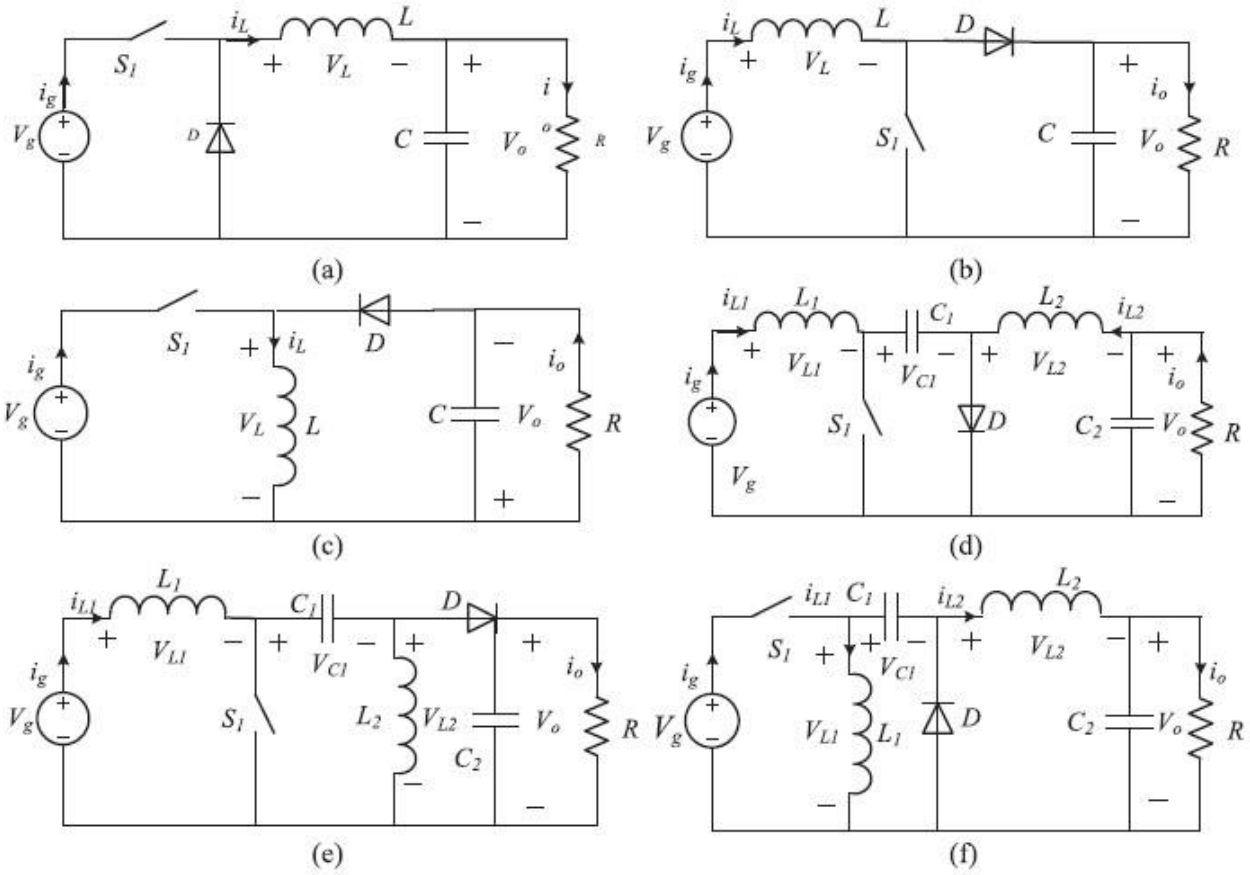

Figure 2: DC-DC converter topologies (a) Buck (b) Boost (c) Buck-Boost (d) Cuk (e) SEPIC (f) Zeta

The topology can be chosen based on the source and operational requirements of LED driver. This paper aims to contribute to the evolving landscape of LED driver design by presenting a comprehensive study on the development and implementation of a specialized driver for a 50W LED lamp. By addressing the intricacies of efficient power regulation, thermal management, and intelligent control features, this research endeavours to provide insights that extend beyond the specific application, laying the groundwork for advancements in LED driver technology applicable across diverse lighting scenarios. As the quest for sustainable and technologically advanced lighting solutions persists, the optimized LED driver discussed herein holds the potential to influence the trajectory of LED lighting towards greater energy efficiency, reliability, and adaptability. The dame design can be extended for Electric Vehicle and microgrid applications with some changes (Bharothu et al., 2022).

2 DESIGN SPECIFICATIONS

The available source in India at the distribution level is 230V, single phase, 50Hz, AC supply. A bridge rectifier is needed to convert the AC signal to unidirectional signal and the average voltage is approximately 207V. The LED lamp operates at a voltage lower than the rectified output. This has to be stepped down to another voltage suitable for LED which makes the necessity of a DC-DC buck converter as shown in Figure 1 (Mrabet et al., 2022; P and

Potnuru, 2023; Rahman et al., 2020; Liu et al., 2018; U.K.Kalla, 2016). The specifications of LED street light considered for the simulation are shown in Table 1.

Table 1 LED Specifications

Parameter	Value
Power	50 W
Voltage	30 V
Current	1.67A

The rectifier output is not a pure DC, so a capacitor to be used to smooth the waveform. Another capacitor and inductor are connected at the load side (LED lamp) to improve the output voltage waveform. The LED lamp is simulated using a resistor. The details of inductor and capacitor used are shown in Table 2.

Table 2 Specification of elements

Element	Value
Capacitance (Rectifier)	15.685uF
Inductor (load side)	5mH
Capacitor (load side)	10.98mF
Resistor (LED)	18 Ω

3 CONTROL SCHEME

The LED needs a constant voltage for better performance. The buck converter is to be controlled for achieving constant voltage. The Pulse width Modulation (PWM) technique is used to control the converter. To further improve the control action and to get good output voltage, a PID controller is also used. The block diagram of the proposed driver is shown in Figure 3. The topology used for the simulation is single stage DC-DC buck converter.

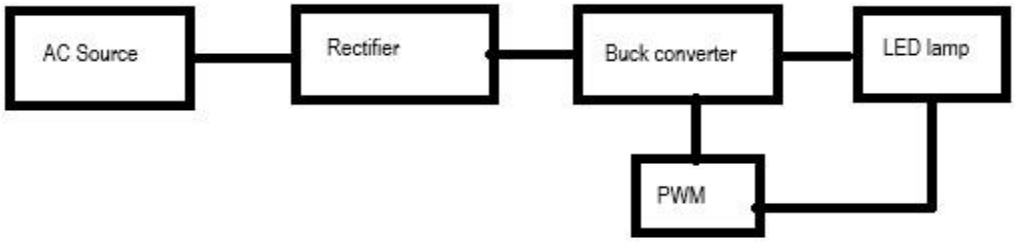

Figure 3: Block diagram of proposed driver

4 SIMULATIONS RESULTS

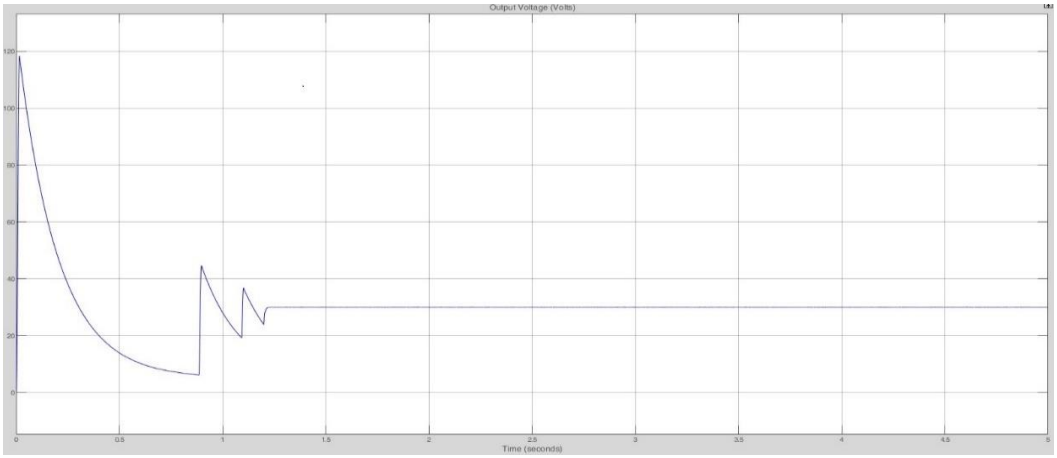

Figure 4: Output voltage

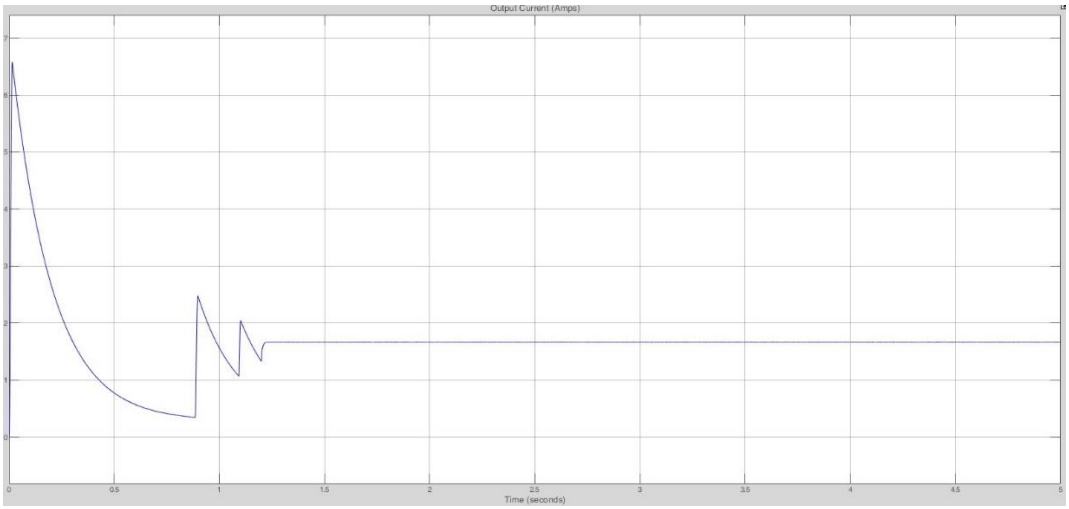

Figure 5: Output current

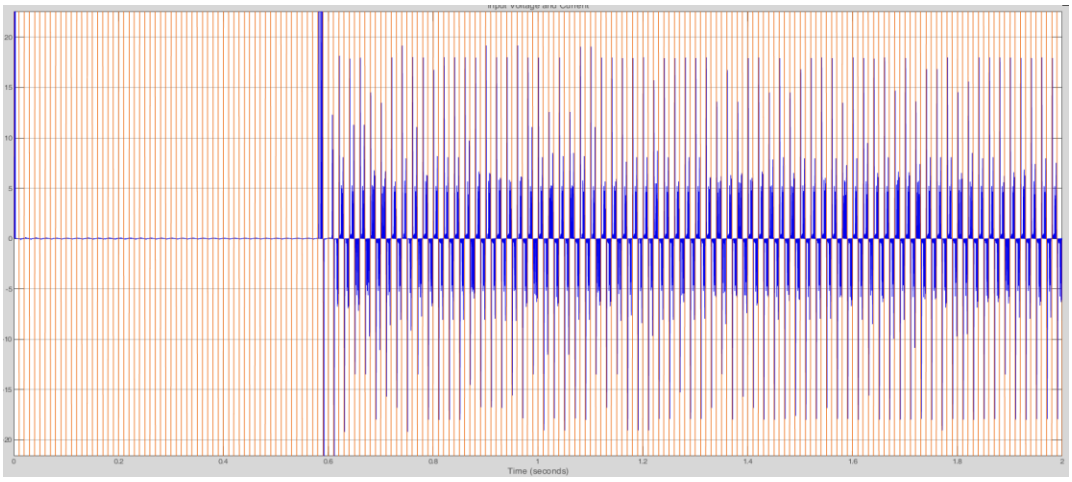

Figure 6: Input voltage and current

From the Figure 6, it is observed that the current wave is not a pure sine wave (distorted waveform), the total harmonic distortion (THD) is high. The THD refers to the alteration or deformation of an electrical waveform from its original pure sine shape. In the MATLAB the THD is found using Fast Fourier transform (FFT) analysis.

5 CONCLUSION

The proposed driver is able to provide a voltage 30V required for the 50W LED lamp. From the results it is found that there is very small ripple in the output voltage and the same can be reduced further by properly choosing gains of PID controller and also the inductor and capacitor. From the input voltage and current waveforms, it is observed that the current waveform is not a pure sinewave (Total Harmonic Distortion (THD) is 252.28%) and the current is not exactly in phase with voltage (phase angle is 9^0 and power factor =0.9877). The performance of the proposed driver can further be improved by reducing THD and increasing power factor. The same driver can be extended to other LEDs but with modifications in the control scheme.

REFERENCES

[1] B. M. Mrabet, A. Chammam, L. Canale and G. Zissis, "Design and Implementation of LEDs Boost Driver for street lighting system," 2021 Joint Conference - 11th International Conference on Energy Efficiency in Domestic Appliances and Lighting & 17th International Symposium on the Science and Technology of Lighting (EEDAL/LS:17), Toulouse, France, 2022, pp. 1-7.

[2] F. J. Nogueira, E. S. Silva, T. S. Gomide, M. F. Braga and H. A. C. Braga, "Design of a transformer less high-power factor low frequency LED driver applied to street lighting," 2015 IEEE 24th International Symposium on Industrial Electronics (ISIE), Buzios, Brazil, 2015, pp. 1172-1177.

[3] H. -C. Kim, M. C. Choi, S. Kim and D. -K. Jeong, "An AC–DC LED Driver With a Two-Parallel Inverted Buck Topology for Reducing the Light Flicker in Lighting Applications to Low-Risk Levels," in IEEE Transactions on Power Electronics, vol. 32, no. 5, pp. 3879-3891, May 2017.

[4] Jyothilal Nayak Bharothu, Madhusudhana Rao B and Krishna P, “A Literature Review on Electrical Nano grids,” Trends in Electrical Engineering, vol.12, pp.1-11, Dec. 2022.

[5] Krishna P and Devendra Potnuru, “A literature review of high gain DC/DC converters,” in Proceedings of National conference on Design Thinking: Trans-disciplinary challenges & opportunities NCDT 2023, Visakhapatnam, July 2023.

[6] Krishna P and Devendra Potnuru, “Power Factor Improvement of Boost PFC Converter for street light applications,” Journal of Power Electronics and Power Systems, vol.13, pp.12-18, Oct. 2023.

[7] Krishna P, “A literature review of non-isolated high gain DC/DC converters,” in Proceedings of International Conference on Emerging Trends in Science, Engineering and Technology ICESET 2023, Vijayawada, February 2023.

[8] M. M. Ali, S. S. Sikander, U. Ali and A. Waleed, "An active Power Factor Correction technique for bridgeless boost AC-DC converter," 2016 International Conference on Intelligent Systems Engineering (ICISE), Islamabad, Pakistan, 2016, pp. 129-134.

[9] N. A. Rahman, K. Kamarudin and R. Baharom, "Boost Active Power Factor Correction Converter Using Various Current Controllers in Double Loop Control Algorithm," 2020 IEEE International Conference on Power and Energy (PECon), Penang, Malaysia, 2020, pp. 24-28.

[10] P. C. V. Luz, M. R. Cosetin, P. E. Bolzan, T. Maboni, M. F. da Silva and R. N. do Prado, "An integrated insulated buck-Flyback converter to feed LED's lamps to street lighting with reduced capacitances," 2015 IEEE International Conference on Industrial Technology (ICIT), Seville, Spain, 2015, pp. 908-913.

[11] S. Uddin, H. Shareef, A. Mohamed, M. A. Hannan and K. Mohamed, "LEDs as energy efficient lighting systems: A detail review," 2011 IEEE Student Conference on Research and Development, Cyberjaya, Malaysia, 2011, pp. 468-472.

[12] U. K. Kalla, "A PFC based control scheme for LED lighting systems," 2016 IEEE 7th Power India International Conference (PIICON), Bikaner, India, 2016, pp. 1-4.

[13] Y. -C. Liu, F. -C. Syu, H. -C. Hsieh, K. A. Kim and H. -J. Chiu, "Hybrid Switched-Inductor Buck PFC Converter for High-Efficiency LED Drivers," in IEEE Transactions on Circuits and Systems II: Express Briefs, vol. 65, no. 8, pp. 1069-1073, Aug. 2018.

[14] Y. Wang, J. M. Alonso and X. Ruan, "A Review of LED Drivers and Related Technologies," in IEEE Transactions on Industrial Electronics, vol. 64, no. 7, pp. 5754-5765, July 2017.